

LATTICE DYNAMICS OF DIAMOND

K. G. Aggarwal

PHY

1966

ARTMENT OF PHYSICS

D

TH
Phy 1966/D

AGGARWAL

Agarwal

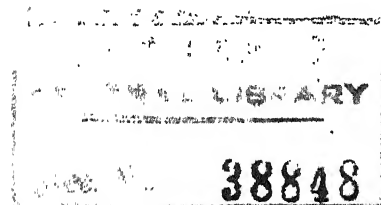
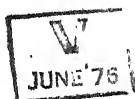
LAT

Indian Institute of Technology, Kanpur

LATTICE DYNAMICS OF DIAMOND

by

KRISHAN GOPAL AGGARWAL



5313
Ag 38 L

Thesis submitted to the Department of Physics, Indian Institute of Technology, Kanpur in partial fulfillment of the requirements of the degree of Doctor of Philosophy

1966

PHY-1966-D-AGG-LAT

Certified that the work presented in this thesis
has been done by Mr. K.G. Aggarwal under my supervision.

J. Mahanty
(J. Mahanty) Sep. 18, 1966
Professor

Department of Physics
Indian Institute of Technology
Kanpur, (INDIA)

VITA

Krishan Gopal Aggarwal was born in Amritsar on July 1, 1940. He did his undergraduate work at Physics Department, Panjab University, Chandigarh and received a Bachelor of Science (Honours School) degree in 1960 and a Master of Science (Honours School) degree in 1961. His subsequent studies and research for this dissertation have been carried out in the Department of Physics of the Indian Institute of Technology, Kanpur. During this period he has held a CSIR junior research fellowship, and subsequently a research assistantship of the Institute. A part of his work has been supported financially by U.S. National Bureau of Standards.

He has three publications:

1. The Frequency Spectra of One-dimensional Lattices; *Ind. J. Pure Appl. Phys.*, 1, 49 (1963).
2. Dynamics and Frequency Distribution Functions for Two Force-Constant Monatomic Linear Chains; *Ind. J. Pure Appl. Phys.*, 3, 324 (1965).
3. The Fourier Expansion Method For Computation of the Frequency Distribution Function of Crystals., *Proc. Phys. Soc.*, 86, 1225 (1965) (Co-authors: J. Mahanty and V.K. Tewary)

ACKNOWLEDGEMENTS

The author is indebted to Professor J. Mahanty for suggesting the problem and for his guidance and encouragement throughout the course of the present work.

The author is thankful to Mr. D.K. Sood for his help in the computational work. The help of Dr. P. Vashishta is acknowledged with gratitude. A special note of appreciation is due to Dr. V.K. Tewary for many a stimulating discussion and for offering his comments and corrections to the manuscript.

It is a pleasure to express appreciation for the hospitality of the Tata Institute of Fundamental Research Bombay, which provided the facilities of the CDC-3600 computer. The author wishes to acknowledge the financial assistance from U.S. National Bureau of Standards. Finally the author wishes to express his gratefulness to Prof. P. Venkateswarlu for his interest in this work.

ABSTRACT

It had previously been established that a Born-von Karman model requires interactions out to at least fifth neighbours to obtain a good fit with the measured dispersion curves for germanium and silicon. In this dissertation a two neighbour Born-von Karman model is applied to the diamond crystal. Out of the five force parameters that occur in the dispersion relations in the (111) direction, only one parameter is kept as free and is fitted with the experimental frequencies at the zone boundaries in the (100) and (111) directions. A good qualitative fit is obtained, which is substantially better than the fit in the case of germanium and silicon with a two neighbour interaction model. To get a better quantitative fit in case of diamond, however, interactions with more distant neighbours should be taken into account.

Secondly, a technique based on the use of Fourier analysis is suggested for the computation of the frequency distribution function of a crystal. The method has been applied to some two- and three-dimensional lattice models for which exact calculations have been done earlier. The present method is seen to yield good agreement with the exact results. It is shown that compared with the usual methods, the Fourier series expansion method saves time and labour and has the added advantage of giving a simple analytic expression for the distribution function. The first fifteen coefficients of the Fourier terms are computed for a number of face-centred and body-centred cubic lattices.

The frequency distribution function of diamond is calculated

using the present technique. The specific heat of diamond is evaluated in the temperature range 0° - 300° K and is seen to agree quite well with the experimental results. Finally the analysis of the dependence of the frequency and amplitude of localised mode due to an isotopic impurity is made.

TABLE OF CONTENTS

| Chapter | Page |
|--|------|
| I. CRITICAL ANALYSIS OF MODELS | 1 |
| II. LATTICE DYNAMICS OF DIAMOND | 25 |
| III. CALCULATION OF FREQUENCY SPECTRA | 50 |
| IV. APPLICATION OF THE FOURIER SERIES EXPANSION METHOD TO DIAMOND | 87 |
| V. CONCLUSION | 99 |
| LITERATURE CITED | 102 |

LIST OF FIGURES

| Figure | Page |
|--------|------|
| 1 | 19 |
| 2 | 26 |
| 3 | 43 |
| 4 | 68 |
| 5 | 73 |
| 6 | 81 |
| 7 | 82 |
| 8 | 90 |
| 9 | 92 |
| 10 | 93 |
| 11 | 97 |

CHAPTER I
CRITICAL ANALYSIS OF MODELS

1. Introduction

The study of lattice vibrations is one of the fundamental disciplines in the theory of solid state. Numerous physical properties of crystals, such as specific heat, electrical and thermal conductivity, scattering of x-rays, electrons and neutrons, infrared absorption, spin-lattice relaxation, Mössbauer effect etc., require for their detailed explanation a knowledge of lattice dynamics of the crystal. New powerful techniques, both theoretical and experimental, have made the study of lattice dynamics all the more interesting. Because of the complex nature of the interatomic forces, about which detailed information is lacking, it is impossible to work out the lattice dynamics of the crystal in an exact way. It is, therefore, essential to resort to various approximate lattice dynamical models for the calculation of the properties of the solids. We outline in this chapter, the salient features of such models.

2. Einstein and Debye Models.

Einstein¹ was one of the first to study lattice dynamics from the standpoint of its bearing on properties of solids. He postulated that a simple crystal could be regarded as an assembly of atomic oscillators each having the same natural frequency ω . At low temperatures, this model predicts the variation of the lattice heat capacity to be as $\exp(-\hbar\omega/KT)$, K being the Boltzmann constant, while the observed variation is of T^3 type; however, at high

temperatures the agreement is good. Debye² and Born and von Karman³ placed lattice dynamics on a more firm footing and showed that a proper evaluation of the vibration frequencies of coupled atomic oscillators leads to better results.

Debye assumed that the lattice vibrates as if it were an elastic isotropic continuum. A maximum frequency ω_D is chosen in order to make the total number of modes equal to the number of classical degrees of freedom. On the basis of this model the specific heat at low temperatures ($T < \theta_D/12$) is proportional to T^3 and reaches its classical value $3NK$ at high temperatures ($\theta_D = \hbar\omega_D/K$ and N = total number of particles in the crystal).

At first Debye theory had remarkable success in representing the variation with temperature of the specific heat of a large number of substances. But later, low temperature calorimetric data definitely revealed that the vibration spectrum of the crystal can be very different from the Debye spectrum. The prime objection to this model is that it ignores the crystal anisotropy and the periodic structure of the crystal which causes it to be a dispersive medium.

⁴ Fuchs introduced the elastic anisotropy in the study of specific heat of lithium. ⁸² Collins has used this anisotropic continuum model for a calculation of the temperature variation of thermal expansion of cubic structures. This model does not, however, give a good representation of the lattice spectrum. The spectrum in this model extends to higher frequencies than that can occur

in a discrete lattice.

3. Born-von Karman Model

The Born-von Karman³ model is based on an exact evaluation of the frequencies for the normal modes of the assembly of coupled atomic oscillators in a crystal. The approach involves cumbersome mathematics and was, therefore, overshadowed by the extremely simple Debye model. Born-von Karman theory went relatively unnoticed till the experiments showed with certainty that Debye's model was insufficient to explain the thermodynamic properties of solids. The plot of Debye characteristic temperature θ , for each value of C_v , against T was not found to be a straight line parallel to the T -axis, as is expected from Debye's theory. Blackman⁵ applied Born-von Karman theory to a linear chain, a two dimensional square lattice and a simple cubic lattice and showed that this theory gives results more nearly like the observed specific heat and emphasized the use of the exact theory as opposed to the approximate method given by Debye, while analysing low temperature specific heat data.

The general theory has been described by several authors (Born and Huang⁶, Peierls⁷, Leibfried⁸, and Maradudin, Montroll and Weiss⁹). We shall give here an outline of this theory and apply it to the case of the diamond crystal in the next chapter.

The basic assumption on which Born-von Karman theory is based is that the nuclear motion in the lattice is determined by an effective potential function Φ which depends only upon the nuclear coordinates.

This implies that the electrons are always able to take up a configuration appropriate to that of the displaced nuclei, and that the change of energy of electrons in the distorted crystal contributes to the effective internuclear potential. Chester¹⁰ has pointed out that the motion of the electrons will be essentially adiabatic, except for those few with the energy close to the Fermi energy. The exclusion principle disallows most of the non-adiabatic transitions.

We consider a three dimensional crystal composed of n unit cells each of which is a parallelepiped bounded by three non-coplanar vectors \underline{a}_1 , \underline{a}_2 and \underline{a}_3 . Each unit cell contains s atoms. We denote the equilibrium position vector of the p th unit cell with respect to a chosen origin by $\underline{r}(p) = p_1 \underline{a}_1 + p_2 \underline{a}_2 + p_3 \underline{a}_3$ (p_1 , p_2 and p_3 are integers), which gives the position of one of its corners and by $\underline{r}(K)$ ($K = 1, 2, 3, \dots, s$) the position vector of the K -th particle in the cell with respect to origin of the cell. Then the position vector of the K -th particle in the p th unit cell shall be written as

$$\underline{r}(pK) = \underline{r}(p) + \underline{r}(K) \quad (1)$$

The total energy $\bar{\Phi}$ can be expanded as a Taylor series in powers of the nuclear displacements $\underline{u}(pK)$ from the equilibrium configuration of the static lattice and in the harmonic approximation it is given by

$$\bar{\Phi} = \bar{\Phi}_0 + \frac{1}{2} \sum_{p,p'} \sum_{K,K'} \sum_{i,j} \bar{\Phi}_{ij}^{(pK, p'K')} u_i(pK) \times u_j(p'K') \quad (2)$$

where $\underline{\Phi}_0$ is the potential energy in the equilibrium configuration and $u_i(pK)$ ($i = x, y, z$) denotes the i th Cartesian component of the displacement $\underline{u}(pK)$ and

$$\underline{\Phi}_{ij}(pK, p'K) = \left. \frac{\partial^2 \underline{\Phi}}{\partial r_i(pK) \partial r_j(p'K)} \right|_0, \quad (3)$$

where subscript 0 signifies that derivatives have been evaluated at the equilibrium positions. It may be noticed that the first order term in the expansion of $\underline{\Phi}$ vanishes since in the equilibrium configuration the force on any particle must vanish. The terms higher than the second order are responsible for thermal conductivity, thermal expansion, and the temperature variation of the elastic constants, as has been mentioned by Leibfriend and Ludwig¹⁰. The equation of motion of the (pK) ion of mass m_K , in the harmonic approximation, is

$$m_K \ddot{u}_i(pK) = - \sum_K \sum_{p'} \sum_j \underline{\Phi}_{ij}(pK, p'K) u_j(p'K) \quad (4)$$

The quantity $\underline{\Phi}_{ij}(pK, p'K)$ thus plays the role of the force constant and represents the force exerted in the i th direction on the atom at $\underline{r}(pK)$ when the atom $\underline{r}(p'K)$ is displaced a unit distance in the j th direction. The periodicity of the lattice requires $\underline{\Phi}_{ij}(pK, p'K)$ to be symmetric in their indices and to depend only on $(p-p')$ rather than p and p' separately:

$$\underline{\Phi}_{ij}(pK, p'K) = \underline{\Phi}_{ji}(p'K, pK) = \underline{\Phi}_{ij}(p-p', K-K). \quad (5)$$

A solution of equation(4) for an independent normal mode of vibration of circular frequency ω and wave number q is

$$u_i(pK) = U_i(K) \exp i(q \cdot r(pK) - \omega t), \quad (6)$$

where $U_i(pK)$ are the amplitudes. Equation(4) leads to

$$\omega^2 m_K U_i(K) = \sum_j \sum_K D_{ij}(q, KK) U_j(K), \quad (7)$$

where

$$D_{ij}(q, KK) = \sum_p \bigoplus_{ij} (pK, pK) \exp i q \cdot (r(pK) - r(pK)) \quad (8)$$

Equation(7) represents a set of 3s homogeneous linear equations for 3s displacements of s atoms in the unit cell. For the existence of a non-trivial solution of these equations, the necessary and sufficient condition is

$$\det \left| \hat{D}(q) - \hat{M} \omega^2 \right| = 0, \quad (9)$$

where $\hat{D}(q)$ is a $3s \times 3s$ matrix, usually called the dynamical matrix, whose elements are the coefficients $D_{ij}(KK, q)$ and \hat{M} is a $3s \times 3s$ diagonal matrix with diagonal elements as m_1, m_2, \dots, m_s . The characteristic equation(9) has $3s$ roots ω_j corresponding to a particular value of the wave number q . Three of these roots, tending to zero as $q \rightarrow 0$, are acoustic branches and the remaining $3s-3$ are optical branches. The values of q are restricted by the cyclic boundary condition (Born and von Karman) ⁶ which requires that for a parallelepiped shaped crystal with its edges parallel to those of the unit cell and having lengths $n_1 a_1, n_2 a_2$ and $n_3 a_3$

$$\exp i \underline{q} \cdot (n_1 \underline{a}_1 + n_2 \underline{a}_2 + n_3 \underline{a}_3) = 1, \quad (10)$$

where n_1, n_2 and n_3 are the number of particles along the three edges of the unit cell. Equation (10) leads to

$$\underline{q} = 2\pi (h_1/n_1 \underline{b}_1 + h_2/n_2 \underline{b}_2 + h_3/n_3 \underline{b}_3), \quad (11)$$

where h_1, h_2 and h_3 are integers and take values from zero through $(n_1 - 1), (n_2 - 1)$ and $(n_3 - 1)$ respectively, and $\underline{b}_1, \underline{b}_2$ and \underline{b}_3 define a reciprocal lattice by the equation

$$\underline{a}_i \cdot \underline{b}_j = S_{ij}. \quad (12)$$

In other words if the unit cell of the reciprocal lattice is subdivided into $n_1 n_2 n_3$ subcells by dividing the three translations into n_1, n_2 and n_3 parts respectively, then $(\underline{q} / 2\pi)$ can only be one of the wave vectors connecting the origin to a point of the subdivision. For large $n (= n_1 n_2 n_3)$, the n distinct values of $(\underline{q} / 2\pi)$ may be regarded as continuously and uniformly distributed in the reciprocal lattice cell.

Recently Lehnert¹¹ et al. have proposed an axially symmetric model which involves lesser number of force constants than the general Born-von Karman model for the same neighbour interaction. This model assumes that the potential energy of the crystal is a sum of bond-stretching and axially symmetric bond-bending terms. The first term is proportional to the square of the component of the relative displacement along $\underline{r}(pK, p'K)$, the vector joining the equilibrium position of two atoms at $\underline{r}(pK)$ and $\underline{r}(p'K)$, and the second term

is proportional to the square of the relative displacement perpendicular to $\underline{r}(pK, p'K)$. The potential energy associated with the atom at (pK) is written as

$$\begin{aligned} \underline{\Phi}_2(pK) = & \frac{1}{2} \sum_p \sum_{K'} \left| \underline{r}(pK, p'K) \right|^{-2} \left[C_S(pp', KK') \right. \\ & \times \left. (\underline{r}(pK, p'K) \cdot \Delta \underline{r}(pK, p'K))^2 \right. \\ & \left. + C_B(pp', KK') (\underline{r}(pK, p'K) \times \Delta \underline{r}(pK, p'K))^2 \right], \quad (13) \end{aligned}$$

where Δ denotes a small displacement operator and C_S and C_B are the bond-stretching and bond-bending force constants between (pK) and $(p'K)$ atoms. From (13) the secular equation is obtained in the usual way and one obtains

$$\hat{D}(KK', \underline{q}) = (\mathcal{D}_{KK'} \sum_{K=1}^s \hat{A}(KK', 0) - \hat{A}(KK', \underline{q})). \quad (14)$$

The elements of $\hat{A}(KK', \underline{q})$ are given by the equation

$$\begin{aligned} \hat{A}_{ij}(KK', \underline{q}) = & \sum_p \left[- \left| \underline{r}(pK, p'K) \right|^{-2} C(pp', KK') \frac{\partial^2}{\partial q_i \partial q_j} \right. \\ & \left. + C_B(pp', KK') \mathcal{D}_{ij} \right] \exp i\underline{q} \cdot \underline{r}(pK, p'K), \quad (15) \end{aligned}$$

$$\text{where } C(pp', KK') = C_S(pp', KK') - C_B(pp', KK'). \quad (16)$$

The subscripts i, j of \underline{q} in equation (15) refer to the Cartesian components of \underline{q} . This model has been applied to copper¹¹, aluminium¹¹ and white tin¹² with success.

The Born-von Karman theory involves a large number of force

constants. The symmetry elements of the crystal structure reduce the number of independent force constants necessary for a general description of the force field appropriate to each class of neighbours. To reduce the number of force constants, one normally assumes short range interaction with the nearest and next-nearest neighbours. In the case of central force interactions with nearest and next-nearest neighbours, the secular equation for a cubic crystal contains only two force constants which can be related to the elastic constants by comparing the secular equation in the long wavelength limit with the corresponding equation of elasticity theory. Now for a cubic crystal, there are three elastic constants. For a unique determination of the force constants, there must be an additional relation between the elastic constants. In this case, the model leads to the Cauchy relation $C_{12} = C_{44}$. Unfortunately Cauchy relation does not hold good for most of the metals. Experimental data on elastic constants show that the values of C_{12} in many cases are as high as two to three times the value of C_{44} .

Fuchs⁴ attributed the failure of Cauchy relation to the presence of the electrons. According to him, certain energies such as ground state energy of the valence electron, Fermi, exchange and the correlation energies of the conduction electrons, depend only on the atomic volume. The forces, arising from these energies, on the displaced ions cannot be regarded as due to the central interaction potential between the ions. They contribute to the compressibility, but do not enter our consideration for strains for which there are no volume changes. The electrons should not, therefore, affect a purely transverse wave. The constants ($C_{11}-C_{12}$) and C_{44} are not affected by the presence of the

electrons, because they are involved in strains where the volume is not changed.

Following the ideas of Fuchs, phenomenological force models have been introduced by the various authors.

4. Phenomenological Force Models Considering Electron Gas

de Launay¹³ has developed a simple model in which the conduction electrons are assumed to behave like an ordinary gas responding in-phase to the longitudinal component of the lattice waves but left unaffected by the transverse components. As the waves travelling in a crystal, in general, are neither purely transverse nor purely longitudinal, they are separated into their longitudinal and transverse components and the electronic effect is assumed to operate in the longitudinal component only. The response modifies the force components so that one set is effective for longitudinal component and a different set for transverse component. For central force interactions with the nearest and next nearest neighbours, the number of parameters that occur in de Launay's model is four, twice the number of parameters occurring in the model without the electron gas modification. These parameters are evaluated from the three elastic constants and the condition that the electron gas does not modify the form of the secular equation for acoustic waves. The new relation that replaces the Cauchy relation is

$$K_c = C_{12} - C_{44}, \quad (17)$$

where K_e is the bulk modulus of the electron gas. From this relation de Launay calculated the number of free electrons per atom for copper and got a reasonable agreement with the experimental value. By comparing the theoretical and experimental $\theta - T$ curves for C_u , de Launay also observed that the electron gas modification is important at low temperatures ($\sim 5^{\circ}\text{K}$)

Bhatia¹⁴ has carried out a similar investigation for cubic lattices. It is assumed that the forces on an ion in the lattice arise from a central interaction which is significant for nearest neighbours only and from certain energies (e.g. Fermi and exchange) which depend on atomic volume only. These energies are due to the free electrons. He is able to introduce three force constants in place of two for the corresponding de Launay model. This he achieved by a suitable choice of a term linear in displacements occurring in the expression for potential. If the exchange interaction term is dropped, the electronic contribution reduces to the one from de Launay's model.

In Bhatia's model

$$\hat{D}_{ii}(q) = \frac{64}{3} (\alpha' + \alpha''/3)(1 - C_1 C_2 C_3) + \frac{4 K_0 a^3 q_i^2}{1 + K_0 q^2 / 4 \pi^2 e^2 n_0^2},$$

$$\hat{D}_{ij}(q) = \frac{64}{9} \alpha'' S_i S_j C_K + \frac{4 K_0 a^3 q_i q_j}{1 + K_0 q^2 / 4 \pi^2 e^2 n_0^2},$$

where

$$\alpha' = \frac{3a}{16} (c_{11} - c_{12}), \quad \alpha'' = \frac{-9a}{16} (c_{11} - c_{12} - 2c_{44}),$$

$$K_0 = c_{11} - c_{44}$$

(b.c.c.) (18a)

and

$$\hat{D}_{ii}(q) = 8\alpha' (3 - c_1 c_2 - c_2 c_3 - c_3 c_1) + 4\alpha'' (2 - c_i c_j - c_i c_K)$$

$$+ \frac{2 K_0 a^3 q_i^2}{1 + K_0 q_i^2 / 4\pi e^2 n_0^2},$$

$$\hat{D}_{ij}(q) = 4\alpha'' S_i S_j + \frac{2 K_0 a^3 q_i q_j}{1 + K_0 q_i^2 / 4\pi e^2 n_0^2},$$

where

$$\alpha' = \frac{a}{4} (c_{11} - c_{12} - c_{44}), \quad \alpha'' = -a (c_{11} - c_{12} - 2c_{44}),$$

$$K_0 = (2c_{11} - c_{12} - 3c_{44}),$$

(f.c.c.) (18b)

where n_0 is the number of electrons per cm^3 and $S_i = \sin(q_i a)$,

$c_i = \cos(q_i a)$ and $2a$ is the lattice constant. q_i is the j th rectangular component of the wave number q .

Bhatia's theory has been successfully applied by Joshi and Homkar¹⁵ for a calculation of the specific heats of a number of

monovalent cubic metals.

A slight variant of de Launay's model has been used by Leibfried and Brenig¹⁶. They have employed an ideal gas in place of Sommerfeld gas used by de Launay. However the results obtained are the same.

Recently Sharma and Joshi¹⁷ have given a semiphenomenological model for lattice waves in metallic crystals. They visualise a metallic crystal as a lattice of bare ions imbedded in a uniform cloud of electrons. The potential between ions is regarded as arising from (1) a central interaction between the ions, which is limited to the nearest and the next nearest neighbours and (2) from certain energies which are due to the compressibility of the conduction electrons and their interaction with the ions. The second effect is averaged over a Wigner-Seitz sphere. They calculated the frequencies of normal modes of sodium in the three symmetry directions and obtained a satisfactory agreement with the results of neutron scattering experiments. This model contains three parameters which are related to the experimentally measured elastic constants. However, the elastic constants used by them have been derived by extrapolation methods.

Recently it has been pointed out by Lax¹⁸ that the phenomenological model of de Launay violates space group symmetry requirements. In a b.c.c. lattice, the points $\pi/a (1,0,0)$ and $\pi/a (0,1,0)$, differing by a reciprocal lattice vector only, should have the same dynamical matrix, but de Launay's model gives an additional term. In this respect the models of Bhatia and that of Sharma and Joshi are also

not physical. Therefore, the success of these models may be considered as a matter of chance.

Krebs¹⁸ has recently given a model that takes care of the symmetry requirements by including Umklapp conditions. The effect of the electrons is considered through the screening parameter of the Coulomb interaction between the ions. The interaction between closed ion shells is included by central interaction between the nearest and next nearest neighbours. This model involves three parameters which are related to the three elastic constants. Krebs used the modified form of screening parameter given by Pines²⁰. The modification was done in a manner suggested by Langor and Vorko²¹. He calculated the dispersion curves for the b.c.c. lattices of Li, Na and K and obtained good agreement with the neutron scattering results. However, there are discrepancies for Li, which according to Krebs are probably due to the failure of free electron approximation for k_F (the wave vector on the Fermi surface). In any case, the agreement will depend on the choice of the screening parameter. Considering the simplicity of this model, it may prove very useful for considering the electron gas effect in metals.

5. Recent Theories:

In the rigorous treatment of the lattice dynamical properties of metals, the main complexity originates from the interaction of conduction electrons with the lattice. The problem is inherently a many body problem with a number of electrons interacting with the

lattice. A general theory of the electron-phonon interaction has been reviewed by Ziman²², Chester²³ and Sham and Ziman²⁴. Novel approaches to the problem have also been discussed by Bardeen and Pines²⁵, Pines²⁰, Migdal²⁶ and Baym²⁷.

Detailed studies of lattice vibrations in metals have been carried out by Toya²⁸. The restrictive conditions imposed in the theory make the applications valid for monovalent metals only. He considers the potential between ions as a sum of (1) the Coulomb repulsion V_a , (2) the ion-electron-ion interaction V_E , which is to include the electron-electron interaction and (3) the sum V_R of the exchange repulsion and Van der Waals attraction. The first two are of long range nature, whereas the third one decreases very rapidly with distance. The contribution V_c is computed by Ewald's method²⁹. To evaluate V_R only the nearest neighbours are taken into account. For V_E Toya used the Hartree-Fock method in the presence of lattice vibrations using a simplified exchange potential due to Slater³⁰. Toya has calculated the vibration frequencies for waves propagating along the symmetry directions of alkali halides and copper. In the case of sodium these results have been compared with the neutron scattering results of Woods et al³¹. They exhibit good agreement except for T_1 branch in (110) direction. Toya's theory takes care of the symmetry properties also. It appears to be the most fundamental one. The trouble, however, in its application is that it contains a number of electronic parameters which are rather difficult to obtain in a precise manner.

Woll and Kohn³² have discussed the theory of the lattice dynamics of metals along similar lines. Their method is a modification of Nakajima's quantum calculation³³ and is essentially a Hartree method, which considers only terms of the first order in both the electron-electron and electron-lattice interactions. However, one cannot place much reliance on a calculation that overlooks the exchange effects and electron correlations.

Efforts have also been made to calculate the atomic force constants from first principles. An early attempt in this field was due to Bronig³⁴. White has calculated the atomic force constants of copper in a more fundamental way using Feynman's theorem³⁵. He used the Koster-Slater formalism³⁶, developed for localised perturbation in crystals, to calculate the change in the conduction electron charge density resulting from the infinitesimal displacement of an ion. Recently Cochran³⁷ has interpreted the force constants of sodium derived by Woods et al.⁴⁴ by using the concept of pseudo-potential for the interaction of conduction electrons with the periodic potential of the lattice³⁸. The calculation is based on the suggestion of Sham³⁹ that the electron-ion interaction potential may be regarded as moving rigidly with the ions in the course of the lattice vibrations and with certain limitations can be used to calculate the matrix elements for the electron-phonon interaction, with the electrons represented by plane waves.

Experimentally the most detailed information on lattice dynamics

has been obtained through the inelastic scattering of thermal and cold neutrons. The use of this technique has helped in establishing, with reasonable accuracy, the dispersion relations for aluminium^{40,41}, copper^{42,43}, sodium⁴⁴, magnesium⁴⁵, beryllium⁴⁶, iron⁴⁷, lead⁴⁸, niobium⁴⁹, tungsten⁵⁰, tantalum⁵¹, nickel⁵², molybdenum⁵³, β -brass⁵⁴, zinc⁵⁵, white tin⁵⁶, diamond⁷², germanium⁶⁷ and silicon⁷⁰.

6. Shell Model

In the last six years some attention has been paid to the shell model. This was originally suggested by Dick and Overhauser⁵⁷ and independently by Hanlon and Lawson⁵⁸ to study the dielectric properties of alkali halides. The first calculation for NaCl was done by Kellerman²⁹ on the basis of Born's theory of ionic crystals. Kellerman treated the ions as point charges and considered the Coulomb interaction between the point charges and a short range repulsive interaction between the first neighbours. The repulsive interaction prevents the lattice from collapsing. Kellerman's calculations fitted well with the experimental value of the frequency of the transverse optical mode of wave number zero. The calculated frequency distribution function also gave reasonable agreement with the specific heat.

Later Kellerman's model was applied to NaI by Woods et al.⁵⁹. The calculated dispersion relations were found to be quite at variance with the experimental results obtained from neutron scattering data. Besides this, Kellerman's model does not explain the dielectric properties of the crystal. Born and Huang⁶ pointed out that the ratio

of the static dielectric constant ϵ_0 to the high frequency dielectric constant ϵ_∞ should be $(\omega_L^2 / \omega_T^2)_{q=0}$. For NaI, Kellermann's model yields the value of this ratio as 3.6 as against the correct value 2.3 from the measured dielectric constant. In this model, the ions are not polarizable and hence there is no possibility of electrons responding to the applied field (which is the only contribution to the dielectric polarization at high frequencies). This model gives, therefore, the values of ϵ_∞ as unity in place of nearly 2.9.

To account for the dielectric properties of alkali halides, Dick and Overhauser introduced the shell model which has been generalised by Cochran⁶⁰. The model assumes each ion to be replaced by a shell of charge Y and a core with charge X , so that the total charge on the ion is $(X+Y)$. Each shell is connected to its own core by an isotropic spring of constant K giving rise to the polarizability $(\epsilon Y)^2 / K$ of the free ion. In addition, there are short range core-core, core-shell and shell-shell interactions. This has been shown in figure 1. The equations of motion are

$$\begin{aligned} \hat{m} \hat{\omega}^2 \underline{U} &= (\hat{R} + \hat{Z} \hat{C} \hat{Z}) \underline{U} + (\hat{T} + \hat{Z} \hat{C} \hat{Y}) \underline{W} \\ 0 &= (\hat{T} + \hat{Y} \hat{C} \hat{Z}) \underline{U} + (\hat{S} + \hat{Y} \hat{C} \hat{Y}) \underline{W}, \end{aligned} \quad (19)$$

where $\hat{R}, \hat{T}, \hat{S}$ are the matrices specifying the short range interactions and \hat{C} is the matrix of Coulomb coefficients. \hat{m}, \hat{Z} and \hat{Y} are diagonal matrices representing the mass, ionic charge, and the charge on the shells respectively. \underline{U} and \underline{W} are vectors; U is the amplitude of the

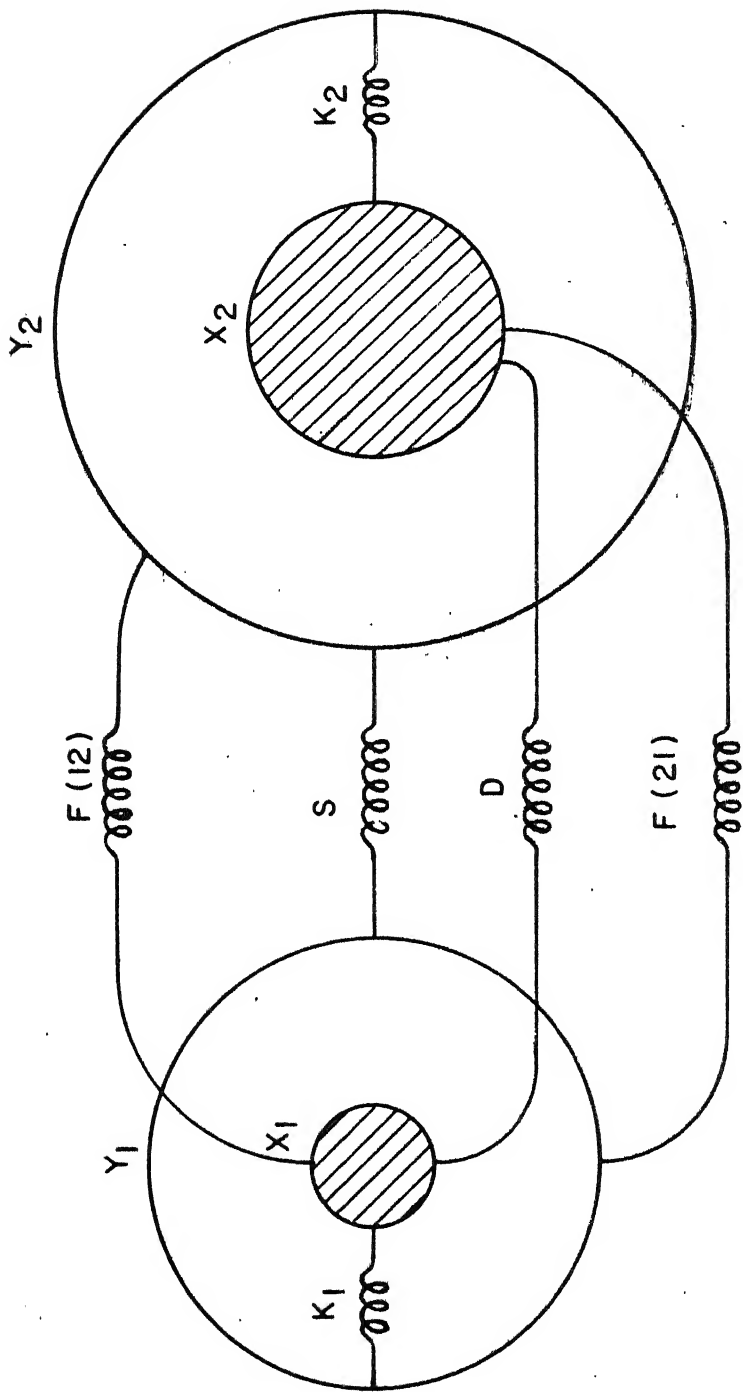


FIG. 1 THE GENERALISED SHELL MODEL DUE TO COCHRAN.

displacements of the ions, while $\hat{Y} W$ represents the electronic dipole moment on the ions. The equations (19), with only nearest neighbour central short range forces, contain seven parameters. This number increases to eight if the ionic charge is considered to be unknown. Woods et al.⁵⁹ have used a simplified version of the model to calculate the dispersion relations for NaI. They considered only the negative ions to be polarizable and the short range interactions were assumed to be operating only through the shells; consequently decreasing the number of parameters to three which were fixed by the elastic constant C_{11} , high and low frequency dielectric constants. The calculations in the symmetry directions were compared with the results of inelastic neutron scattering experiments and with the predictions of the rigid ion model. Even a simplified shell model was seen to give much better agreement (Root mean - square deviation $\approx 7\%$) with the experimental results than the point ion model. The largest deviation is near the zone boundary in the (111) direction. Woods et al. have also shown that the discrepancy cannot be removed, without worsening the agreement at other places, by simple introduction of second neighbour interaction. Serious discrepancies occur for the longitudinal optical modes (deviation is as high as 20% near the zone boundary). To remove such discrepancies, Cowley et al.⁶¹ have studied six different simplified versions of the more generalized Cochran's shell model and calculated the dispersion relations for NaI and KBr. The parameters were evaluated by a least squares fit to the measured dispersion curves in the three symmetry directions, the high and low

frequency dielectric constants and the elastic constants. The maximum number of parameters was reduced to ten by limiting the short range interactions to the second neighbours and the ad hoc assumption that the short range interactions are through shells.

In a nutshell, the six models can be listed in the order of increasing complexity as follows. (Each includes the features of the previous one).

- 1) Only negative ions are polarizable and only central nearest neighbour short range forces are included.
- 2) Central second nearest neighbour and noncentral nearest neighbour forces are included.
- 3) Ionic charge is allowed to vary.
- 4) The polarizability of the positive ions is introduced assuming the shell charge to be the same for both the ions.
- 5) Positive ion polarizability is introduced in an alternative way. The electrical polarizability of the ion is fixed to its quoted value⁶.
- 6) All the ten parameters are allowed to vary. These include five short range interaction parameters, two crystal polarizabilities, two short range polarizabilities and the ionic charge Z.

Out of all these, only the sixth model gave good fit to the elastic and dielectric constants and to the dispersion curves in the symmetry directions. However, the difficulty with this model is that the short range polarizability of the positive ions turns out to be negative for both KBr and NaI. On the basis of shell model it implies

that either the shell charges are positive or the spring constants are negative, which is clearly unphysical. Cowley et al.⁶¹ have suggested that the inclusion of quadrupole moments may improve the matters.

The same type of calculations, without using the shell model conception, have also been carried out by Tolpygo and co-workers^{62,63} and Hardy^{64,65}. They considered the dipole moments and took into account the fact that the dipole moment is determined by the long range as well as short range interactions. Cowley et al.⁶¹ have shown that Hardy's calculations are essentially the same as obtained by them, except that Hardy neglected a term that specifies short range interaction on an ion by the neighbouring dipoles. The theory of Tolpygo and co-workers is also identical with the shell model theory, apart from the neglect of short range dipole-dipole forces in their theory.

7. Lattice Dynamics of Covalent Crystals

The situation in covalent crystals is still more obscure. Hsieh calculated the dispersion relations of germanium using a simple Born-von Karman model with non-central first neighbour and central second neighbour interactions. When these were compared with the results of inelastic neutron scattering experiments⁶⁷, the agreement turned out to be very poor, particularly for the frequencies of the transverse acoustic modes where the discrepancy was as high as 70%. Herman⁶⁸ demonstrated that by going to interactions upto fifth neighbours and

beyond (a fifth neighbour model has sixteen parameters, but only 15 occur in the dispersion relations in the symmetry directions), it is possible to obtain force models which fit the elastic constants and the experimental frequencies within the experimental error. This implies that forces of very long range are present. Lax⁶⁹ suggested that this long range nature of the forces probably originates from the quadrupole-quadrupole interaction that arises due to the distortion and compression of the valence electron distribution.

Cochran⁶⁰ studied the lattice dynamics of germanium on the basis of shell model, which accounts for the long range forces by including the interaction between electrical dipole moments induced on the atoms when they are displaced from their equilibrium positions. He considered the interactions with nearest neighbours, involving six short range force constants, the isotropic core-shell constant K and the shell charge Z . The polarizability was expressed in terms of the latter two parameters and the dispersion relations were written in such a way that only seven independent parameters occurred, with polarizability as one of them. Cochran further reduced the number of parameters to five by putting an arbitrary restriction that the ratio of the x y force constant to x x force constant is the same for the shell-shell interaction, bonding interaction between a shell and the surrounding atoms and the interaction between the rigid atoms. Two of the remaining parameters were fixed by the elastic constants and the third was fixed by the dielectric constant. The remaining two parameters were adjusted to fit the experimental frequencies at the

centre and zone boundaries in (100) and (111) directions. The agreement in general is quite good except for the longitudinal acoustic nodes of short wavelength, where the discrepancy is about 14%.

Recently Dolling⁷⁰ used the shell model to fit the dispersion curves of silicon and germanium. He found that a second neighbour model involving eleven parameters was required to obtain a quantitative fit. A generalised second neighbour shell model contains nineteen parameters. Dolling reduced this number to eleven by imposing somewhat arbitrary restrictions.

The shell model has evidently proved useful in the case of alkali halides, germanium and silicon. The main drawback is the large number of parameters involved. For the NaCl structure, even the first neighbour interactions involve eleven parameters. In the diamond structure, the nearest neighbour interactions result in eight parameters and the inclusion of second nearest neighbour interactions leads to nineteen parameters. The number of parameters, of course, has been reduced in the various cases but not without arbitrary restrictions. These considerations have instigated the author to study the lattice dynamics of diamond on the basis of simple Born-von Karman model rather than the shell model. The dispersion relations are given in the next chapter.

CHAPTER II

LATTICE DYNAMICS OF DIAMOND

1. Model for Diamond

It has previously been demonstrated by Herman⁶⁸ that for germanium interactions with at least five nearest neighbours are required in order to get a good fit with the results from neutron scattering data. The same is true for silicon, as the dispersion curves for silicon and germanium are homologous⁷¹. So many neighbours are needed probably because the transverse acoustic branches of germanium and silicon are very much flat near the zone boundary. But for diamond this is not the case⁷². One might expect a simpler Born-von Karman model to give a reasonable fit with the experimental curves. The shell model can also be tried, but the large number of parameters prevents us from drawing any conclusions.

With this point in view, calculations with a second neighbour Born-von Karman model, with the values of elastic constants and the Raman frequency as constraints, are presented here. In the following section, dispersion relations for diamond are derived. Though it has been done previously,^{73,74,68} it is repeated here in order to explain the notation for later reference and to elaborate on the force constant matrices for the second neighbour interaction.

2. Force Constant Matrices for Diamond

The diamond lattice (fig. 2) is composed of identical particles, lying on two equivalent interpenetrating face-centred cubic lattices. One of the lattices is displaced one quarter of the distance

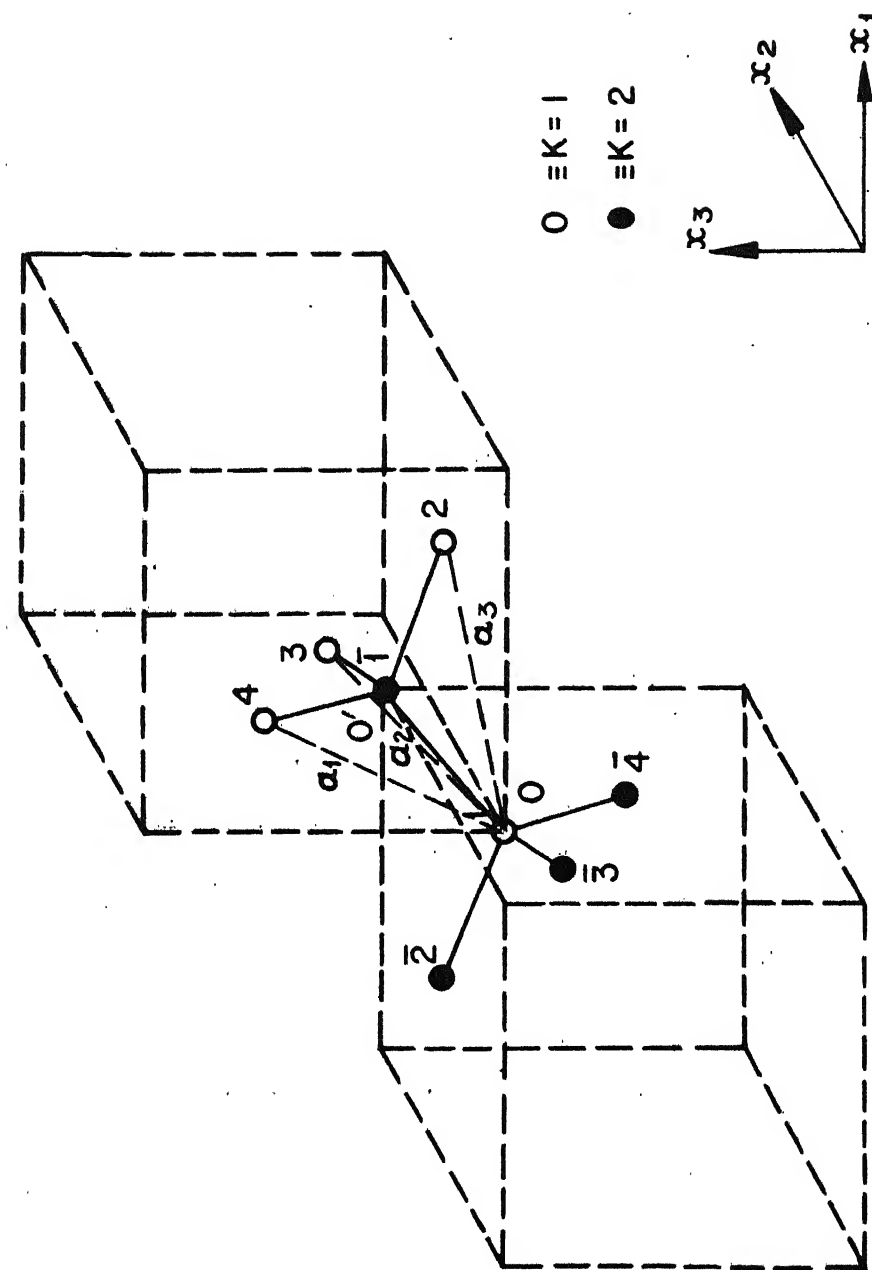


FIG. 2 FIRST NEIGHBOURS OF THE TWO CARBON ATOMS IN THE UNIT CELL OF DIAMOND.

TABLE 1

| | x_1 | x_2 | x_3 | K | p | p_1 | p_2 | p_3 | KK |
|--|--------|--------|--------|-----|-----------|-------|-------|-------|------|
| First neighbours of 0 ($K' = 1$) | $a/2$ | $a/2$ | $a/2$ | 2 | $\bar{1}$ | 0 | 0 | 0 | 21 |
| | $-a/2$ | $-a/2$ | $a/2$ | 2 | $\bar{2}$ | 0 | 0 | -1 | 21 |
| | $-a/2$ | $-a/2$ | $-a/2$ | 2 | $\bar{3}$ | 0 | -1 | 0 | 21 |
| | $a/2$ | $-a/2$ | $-a/2$ | 2 | $\bar{4}$ | -1 | 0 | 0 | 21 |
| First neighbours of 0 ($K' = 2$) | 0 | 0 | 0 | 1 | 1 | 0 | 0 | 0 | 12 |
| | a | a | 0 | 1 | 2 | 0 | 0 | 1 | 12 |
| | a | 0 | a | 1 | 3 | 0 | 1 | 0 | 12 |
| | 0 | a | a | 1 | 4 | 1 | 0 | 0 | 12 |

along the cube diagonal of the other. Thus, there are two particles in the primitive unit cell, one on each of the face-centred lattices. Referred to a rectangular co-ordinate system with origin at a lattice point, the cell vectors of the lattice are

$$\underline{a}_1 = a (0,1,1), \underline{a}_2 = a (1,0,1), \underline{a}_3 = a (1,1,0), \quad (20)$$

where $2a$ is the lattice constant of diamond ($= 3.56 \times 10^{-8}$ cm.). The position vector of the equilibrium position of any particle in the lattice is given by equation (1). For diamond lattice the origin can be chosen such that

$$\underline{r}(01) = (0,0,0); \underline{r}(02) = a (\frac{1}{2}, \frac{1}{2}, \frac{1}{2}) \quad (21)$$

TABLE 2 (a)

| Second neighbours of 0 | | | | | Second neighbours of 0 | | | | |
|------------------------|-------|-------|---|----|------------------------|-----------------|-----------------|---|----|
| x_1 | x_2 | x_3 | K | p | x_1 | x_2 | x_3 | K | p |
| 0 | a | a | 1 | 5 | $\frac{1}{2}a$ | $-\frac{1}{2}a$ | $-\frac{1}{2}a$ | 2 | 5 |
| 0 | a | -a | 1 | 6 | $\frac{1}{2}a$ | $-\frac{1}{2}a$ | $\frac{3}{2}a$ | 2 | 6 |
| a | 0 | a | 1 | 7 | $-\frac{1}{2}a$ | $\frac{1}{2}a$ | $-\frac{1}{2}a$ | 2 | 7 |
| -a | 0 | a | 1 | 8 | $\frac{3}{2}a$ | $\frac{1}{2}a$ | $-\frac{1}{2}a$ | 2 | 8 |
| a | a | 0 | 1 | 9 | $-\frac{1}{2}a$ | $-\frac{1}{2}a$ | $\frac{1}{2}a$ | 2 | 9 |
| a | -a | 0 | 1 | 10 | $-\frac{1}{2}a$ | $\frac{3}{2}a$ | $\frac{1}{2}a$ | 2 | 10 |
| 0 | -a | -a | 1 | 11 | $\frac{1}{2}a$ | $\frac{3}{2}a$ | $\frac{3}{2}a$ | 2 | 11 |
| 0 | -a | a | 1 | 12 | $\frac{1}{2}a$ | $\frac{3}{2}a$ | $-\frac{1}{2}a$ | 2 | 12 |
| -a | 0 | -a | 1 | 13 | $\frac{3}{2}a$ | $\frac{1}{2}a$ | $\frac{3}{2}a$ | 2 | 13 |
| -a | 0 | -a | 1 | 14 | $-\frac{1}{2}a$ | $\frac{1}{2}a$ | $\frac{3}{2}a$ | 2 | 14 |
| -a | -a | 0 | 1 | 15 | $\frac{3}{2}a$ | $\frac{3}{2}a$ | $\frac{1}{2}a$ | 2 | 15 |
| -a | a | 0 | 1 | 16 | $\frac{3}{2}a$ | $-\frac{1}{2}a$ | $\frac{1}{2}a$ | 2 | 16 |

TABLE 2 (b)

These atoms are labelled as 0 and $0'$ in the figure 2. Atoms lying on the same cubic lattice as 0 are labelled $K = 1$, and those lying on the same cubic lattice as $0'$ are labelled $K = 2$. Each atom has four nearest neighbours arranged tetrahedrally at a distance $a\sqrt{3}/2$ and twelve next nearest neighbours at a distance $a\sqrt{2}$, lying on the same face-centred cubic lattice.

Tables 1, 2(a) and 2(b) give the coordinates, the corresponding numbers p and K and the integers (p_1, p_2, p_3) , of the nearest and next nearest neighbours of 0 and $0'$.

For calculating the dispersion relation, the force constants as defined by equation (3) are required. Now all of these force constants are not independent. In fact, the number of independent force constants comes out to be considerably small if one exploits the symmetry of the lattice. For example, the translational symmetry gives the relation (5). All the force constants are given by 3×3 force constant matrices between one nucleus, which can be chosen at the origin, and the other nuclei in the crystal. The force constants behave as covariant tensors of the second rank with respect to the coordinate transformations. In order to find the relations that exist between the elements of force constant matrices, all those symmetry operations which will bring the lattice into self-coincidence have to be applied. The number and nature of these operations are determined by the space group of the lattice. They comprise rotations, reflections, glide planes and combinations of these. If a symmetry operation is expressed as a transformation

matrix \hat{T} , then

$$\underline{r} (P K) = \hat{T} \underline{r} (p k), \quad (22)$$

where $\underline{r} (p k)$ and $\underline{r} (P K)$ are two lattice points. The elements of the matrix $\hat{D} (pk, p'k')$ will then have the transformation law⁷⁵

$$\hat{D} (P K, P'K') = \hat{T} \hat{D} (pk, p'k') \hat{T}^T, \quad (23)$$

where \hat{T}^T is the transpose of \hat{T} and the change of indices is obtained from (22).

The symmetry operations of the diamond lattice can be described by six transformation matrices⁷³ as given below,

(i) A_1 : A three-fold axis of rotation, $x_1 = x_2 = x_3$, represented by the matrix

$$\hat{T}_1 = \begin{bmatrix} 0 & 1 & 0 \\ 0 & 0 & 1 \\ 1 & 0 & 0 \end{bmatrix} \quad (24a)$$

(ii) A_2 : A centre of inversion at the point $x_1 = x_2 = x_3 = a/4$; this is equivalent to a centre of inversion at $(0,0,0)$ and a translation $x_1 = x_2 = x_3 = a/2$. The latter affects only the change of label, and the \hat{T} -matrix is, therefore, that due to the inversion at $(0,0,0)$, i.e.,

$$\hat{T}_2 = \begin{bmatrix} -1 & 0 & 0 \\ 0 & -1 & 0 \end{bmatrix} \quad (24b)$$

(iii) A_3 : Three planes of reflection : one is $x_1 = x_2$ giving the matrix

$$\hat{T}_3 = \begin{bmatrix} 0 & 1 & 0 \\ 1 & 0 & 0 \\ 0 & 0 & 1 \end{bmatrix} \quad (24c)$$

The other two planes of reflection $x_2 = x_3$ and $x_3 = x_1$ can be obtained from A_1 and A_3 .

(iv) A_4 : A rotation through $\pi/2$ about an axis through the point $a(\frac{1}{2}, \frac{1}{2}, \frac{1}{2})$ parallel to the x_3 -axis followed by a rotation through $\pi/2$ about an axis through the same point parallel to the x_1 -axis, represented by the matrix

$$\hat{T}_4 = \begin{bmatrix} 0 & -1 & 0 \\ 0 & 0 & -1 \\ 1 & 0 & 0 \end{bmatrix} \quad (24d)$$

(v) A_5 : A rotation through $\pi/2$ about an axis parallel to the x_1 -axis through the point $a(\frac{1}{2}, \frac{1}{2}, \frac{1}{2})$ followed by a rotation through $\pi/2$ about an axis through the same point parallel to the x_2 -axis, with the corresponding matrix

$$\hat{T}_5 = \begin{bmatrix} 0 & 1 & 0 \\ 0 & 0 & -1 \\ -1 & 0 & 0 \end{bmatrix} \quad (24e)$$

(vi) A_6 : A rotation through $\pi/2$ about an axis parallel to the x_2 -axis through the point $a(\frac{1}{2}, \frac{1}{2}, \frac{1}{2})$ followed by a rotation through $\pi/2$ about an axis through the same point parallel to the x_3 -axis, giving

$$\hat{T}_6 = \begin{bmatrix} 0 & -1 & 0 \\ 0 & 0 & 1 \\ -1 & 0 & 0 \end{bmatrix} \quad (24f)$$

In addition, there are symmetry conditions given by equation (5).

$\hat{D}^p_{(p, KK')}$ may be represented by \hat{D}^p where the superscript p denotes a particular choice of p , K and K' . In order to use the formula (23) the change of indices p must also be specified. This is given by equation (22) and is concisely put in table 3 in the notation of the substitution groups. In this table by (a, b, c) etc. we mean that a matrix with a certain number in a cycle is to be derived from the matrix with the number following it in the cycle by the operation $\hat{T} \xrightarrow{a} \hat{T}$ i.e. $\hat{D}^a = \hat{T} \hat{D}^b \hat{T}$. Thus from A_2 , we obtain

$$\hat{D}^p = \hat{T}_2 \hat{D}^p \hat{T}_2 = \hat{D}^p, \quad p = 1, 16 \quad (25)$$

From A_1 and A_3 , since \hat{D}^1 is invariant with respect to \hat{T}_1 and \hat{T}_3 , we have

$$\hat{D}_{11}^1 = \hat{D}_{22}^1 = \hat{D}_{33}^1, \quad \hat{D}_{12}^1 = \hat{D}_{13}^1 = \hat{D}_{23}^1 = \hat{D}_{21}^1 = \hat{D}_{31}^1 = \hat{D}_{32}^1$$

TABLE 3
Symmetry operations in the diamond lattice

| Symmetry operator | Change of label p |
|-------------------|--|
| A_1 | (1)(2,4,3)(5,7,9)(6,8,10)(15,11,13)(16,12,14) (\bar{1})(\bar{2},\bar{4},\bar{3})(\bar{5},\bar{7},\bar{9})(\bar{6},\bar{8},\bar{10})(\bar{15},\bar{11},\bar{13})(\bar{16},\bar{12},\bar{14}) |
| A_2 | (\bar{1},1)(\bar{2},2)(\bar{3},3)(\bar{4},4)(\bar{5},5)(\bar{6},6)(\bar{7},7)(\bar{8},8)(\bar{9},9) (\bar{10},10)(\bar{11},11)(\bar{12},12)(\bar{13},13)(\bar{14},14)(\bar{15},15)(\bar{16},16) |
| A_3 | (1)(2)(4,3)(7,5)(14,6)(12,8)(9)(16,10)(13,11)(15) (\bar{1})(\bar{2})(\bar{4},\bar{3})(\bar{7},\bar{5})(\bar{14},\bar{6})(\bar{12},\bar{8})(\bar{9})(\bar{16},\bar{10})(\bar{13},\bar{11})(\bar{15}) |
| A_4 | (3)(1,4,2)(14,15,5)(13,16,6)(10,12,7)(11,8,9) (\bar{3})(\bar{1},\bar{4},\bar{2})(\bar{14},\bar{15},\bar{5})(\bar{13},\bar{16},\bar{6})(\bar{10},\bar{12},\bar{7})(\bar{11},\bar{8},\bar{9}) |
| A_5 | (2)(3,4,1)(10,5,13)(9,6,14)(11,7,16)(12,8,15) (\bar{2})(\bar{3},\bar{4},\bar{1})(\bar{10},\bar{5},\bar{13})(\bar{9},\bar{6},\bar{14})(\bar{11},\bar{7},\bar{16})(\bar{12},\bar{8},\bar{15}) |
| A_6 | (4)(2,3,1)(16,5,8)(15,6,7)(13,9,12)(14,10,11) (\bar{4})(\bar{2},\bar{3},\bar{1})(\bar{16},\bar{5},\bar{8})(\bar{15},\bar{6},\bar{7})(\bar{13},\bar{9},\bar{12})(\bar{14},\bar{10},\bar{11}) |

Hence, we may put

$$\left. \begin{array}{c} \hat{D}^1 \\ \hat{D}^1 \end{array} \right\} = - \begin{bmatrix} \alpha & \beta & \beta \\ \beta & \alpha & \beta \\ \beta & \beta & \alpha \end{bmatrix} \quad (26a)$$

where m is the mass of the carbon atom. From A_4 we obtain,

$$\hat{D}^1 = \hat{T}_4 \hat{D}^4 \hat{T}_4 \sim$$

This gives us

$$\left. \begin{array}{c} \hat{D}^4 \\ \hat{D}^4 \end{array} \right\} = - \begin{bmatrix} \alpha & -\beta & -\beta \\ -\beta & \alpha & \beta \\ -\beta & \beta & \alpha \end{bmatrix} \quad (26b)$$

By repeated application of A_1 we find

$$\left. \begin{array}{c} \hat{D}^2 \\ \hat{D}^2 \end{array} \right\} = \hat{T}_1 \hat{D}^4 \hat{T}_1 \sim = - \begin{bmatrix} \alpha & \beta & -\beta \\ \beta & \alpha & -\beta \\ -\beta & -\beta & \alpha \end{bmatrix} \quad (26c)$$

and

$$\left. \begin{array}{c} \hat{D}^3 \\ \hat{D}^3 \end{array} \right\} = \hat{T}_1 \hat{D}^2 \hat{T}_1 \sim = - \begin{bmatrix} \alpha & -\beta & \beta \\ -\beta & \alpha & -\beta \\ \beta & -\beta & \alpha \end{bmatrix} \quad (26d)$$

From A_3 , since \hat{D}^9 is invariant with respect to \hat{T}_3 ,

$$\hat{D}_{11}^9 = \hat{D}_{22}^9, \hat{D}_{12}^9 = \hat{D}_{21}^9, \hat{D}_{13}^9 = \hat{D}_{23}^9, \text{ and } \hat{D}_{31}^9 = \hat{D}_{32}^9.$$

Therefore, we may write

$$\hat{D}^9 = - \begin{bmatrix} \mu & \nu & \delta \\ \nu & \mu & \delta \\ \delta' & \delta' & \lambda \end{bmatrix} \quad (27)$$

Now table (2b) shows that for the second neighbours $K_1 = K_2 = 1$ or 2, and the integers (p_1, p_2, p_3) for the atoms P and $(P + 6)$ differ just by a negative sign. This, with the help of (5), permits us to write

$$\hat{D}^P = \hat{D}^{P+6}, \quad P = 5 \text{ through } 10. \quad (28)$$

Thus we obtain from (27) and (28),

$$\hat{D}^{15} = - \begin{bmatrix} \mu & \nu & \delta' \\ \nu & \mu & \delta' \\ \delta & \delta & \lambda \end{bmatrix} \quad (29)$$

Also, A_4 yields,

$$\hat{D}^8 = \hat{T}_4 \hat{D}^9 \hat{T}_4 = - \frac{1}{m} \begin{bmatrix} \mu & \delta & -\nu \\ \delta' & \lambda & -\delta' \\ -\nu & -\delta & \mu \end{bmatrix} \quad (30)$$

From A_5 we obtain

$$\hat{D}^{15} = \hat{T}_5 \hat{D}^8 \hat{T}_5 = - \begin{bmatrix} \mu & \nu & -\delta \\ \nu & \mu & -\delta \\ -\delta' & -\delta' & \lambda \end{bmatrix} \quad (31)$$

The comparison of (29) and (31) shows

$$\delta' = -\delta \quad (32)$$

Here it may be mentioned that Smith⁷³ had incorrectly assumed the

force constant matrices for the second neighbours to be symmetric and hence chose \hat{D} as zero. This was, to the author's knowledge, first mentioned by Saint James⁷⁴.

By repeated application of A_1 we obtain the matrices \hat{D}^7 , \hat{D}^5 , \hat{D}^6 and \hat{D}^{10} . The use of (25) and (28) gives us the rest of the matrices. Lastly the matrix \hat{D}^0 is obtained by noting that the potential energy Φ is invariant under rigid translations and rotations and hence

$$\sum_{p', K'} \hat{D}_{ij} (p', K K') = 0 \quad \quad (33)$$

Therefore,

$$\hat{D}_{ij} (0, K K) = - \sum'_{p', K'} \hat{D}_{ij} (p', K K'), \quad \quad (34)$$

where the prime on the summation sign indicates that the term with $p' = 0, K = K'$ is omitted.

Table 4 depicts all the force constant matrices.

TABLE 4

Force constant matrices for the first two neighbours in diamond lattice.

$$\hat{D}^1 = \hat{D}^{\bar{1}} = - \begin{bmatrix} \alpha & \beta & \beta \\ \beta & \alpha & \beta \\ \beta & \beta & \alpha \end{bmatrix}, \quad \hat{D}^2 = \hat{D}^{\bar{2}} = - \begin{bmatrix} \alpha & \beta & -\beta \\ \beta & \alpha & -\beta \\ -\beta & -\beta & \alpha \end{bmatrix}$$

$$\hat{D}^3 = \hat{D}^{\bar{3}} = - \begin{bmatrix} \alpha & -\beta & \beta \\ -\beta & \alpha & -\beta \\ \beta & -\beta & \alpha \end{bmatrix}, \quad \hat{D}^4 = \hat{D}^{\bar{4}} = - \begin{bmatrix} \alpha & -\beta & -\beta \\ -\beta & \alpha & \beta \\ -\beta & \beta & \alpha \end{bmatrix}$$

$$\hat{D}^5 = \hat{D}^{\bar{5}} = \hat{D}^{11} = \hat{D}^{\bar{11}} = - \begin{bmatrix} \lambda & -\delta & -\delta \\ \delta & \mu & \nu \\ \delta & \nu & \mu \end{bmatrix}, \quad \hat{D}^6 = \hat{D}^{\bar{6}} = \hat{D}^{12} = \hat{D}^{\bar{12}} = - \begin{bmatrix} \lambda & \delta & -\delta \\ -\delta & \mu & \nu \\ \delta & \nu & \mu \end{bmatrix}$$

$$\hat{D}^7 = \hat{D}^{\bar{7}} = \hat{D}^{13} = \hat{D}^{\bar{13}} = - \begin{bmatrix} \mu & \delta & \nu \\ -\delta & \lambda & -\delta \\ -\nu & \delta & \mu \end{bmatrix}, \quad \hat{D}^8 = \hat{D}^{\bar{8}} = \hat{D}^{14} = \hat{D}^{\bar{14}} = - \begin{bmatrix} \mu & \delta & -\nu \\ -\delta & \lambda & \delta \\ -\nu & -\delta & \mu \end{bmatrix}$$

$$\hat{D}^9 = \hat{D}^{\bar{9}} = \hat{D}^{15} = \hat{D}^{\bar{15}} = - \begin{bmatrix} \mu & \nu & \delta \\ \nu & \mu & \delta \\ -\delta & -\delta & \lambda \end{bmatrix}, \quad \hat{D}^{10} = \hat{D}^{\bar{10}} = \hat{D}^{16} = \hat{D}^{\bar{16}} = - \begin{bmatrix} \mu & -\nu & -\delta \\ -\nu & \mu & \delta \\ \delta & \delta & \lambda \end{bmatrix}$$

$$D(0,11) = D(0,22) = {}^4\alpha \begin{bmatrix} 1 & 0 & 0 \\ 0 & 1 & 0 \\ 0 & 0 & 1 \end{bmatrix} + 4(\lambda + 2\mu) \begin{bmatrix} 1 & 0 & 0 \\ 0 & 1 & 0 \\ 0 & 0 & 1 \end{bmatrix}$$

3. Secular Equation

The elements of the matrix $\hat{D}(q)$ in (9) are obtained by a simple substitution of $\hat{D}(pk, pk')$, which is represented by \hat{D}^P and given in table 5, and the corresponding coordinates of the different neighbours from tables 1 and 2. Then the summation in equation (8) is carried out over the different atoms and the corresponding elements of the dynamical matrix evaluated. For the model of diamond we have chosen, these are

$$\hat{D}_{11}(11) = \hat{D}_{11}(22) = 4 \left[\alpha + \lambda (1 - c_y c_z) + \mu (2 - c_x c_y - c_z c_x) \right],$$

$$\hat{D}_{22}(11) = \hat{D}_{22}(22) = 4 \left[\alpha + \lambda (1 - c_z c_x) + \mu (2 - c_y c_z - c_x c_y) \right],$$

$$\hat{D}_{33}(11) = \hat{D}_{33}(22) = 4 \left[\alpha + \lambda (1 - c_x c_y) + \mu (2 - c_z c_x - c_y c_z) \right] ,$$

$$\hat{D}_{12}(11) = \hat{D}_{12}^*(22) = 4 \nu s_x s_y - 4 i \delta s_z (c_x - c_y) ,$$

$$\hat{D}_{23}(11) = \hat{D}_{23}^*(22) = 4 \nu s_z s_y - i 4 \delta s_x (c_y - c_z) ,$$

$$\hat{D}_{13}(11) = \hat{D}_{13}^*(22) = 4 \nu s_z s_x + i 4 \delta s_y (c_z - c_x) ,$$

$$\hat{D}_{11}(12) = \hat{D}_{22}(12) = \hat{D}_{33}(12)$$

$$= -\alpha \left[1 + \exp - i \pi (q_x + q_y) + \exp - i \pi (q_y + q_z) \right. \\ \left. + \exp - i \pi (q_z + q_x) \right] ,$$

$$\hat{D}_{12}(12) = \hat{D}_{21}(12) = -\beta \left[1 + \exp - i \pi (q_x + q_y) \right.$$

$$\left. - \exp - i \pi (q_y + q_z) - \exp - i \pi (q_z + q_x) \right] ,$$

$$\hat{D}_{23}(12) = \hat{D}_{32}(12) = -\beta \left[1 - \exp - i \pi (q_x + q_y) \right. \\ \left. + \exp - i \pi (q_y + q_z) - \exp - i \pi (q_z + q_x) \right] ,$$

and

$$\hat{D}_{13}(12) = \hat{D}_{31}(12) = -\beta \left[1 - \exp - i \pi (q_x + q_y) \right. \\ \left. - \exp - i \pi (q_y + q_z) + \exp - i \pi (q_z + q_x) \right] , \quad (35)$$

where $C_x = \cos(\pi q_x)$, $S_x = \sin(\pi q_x)$ and $(\pi q_x/a)$ is the x-component of the wave number q . The remaining elements are obtained by using the Hermitian property of the dynamical matrix.

4. Dispersion Curves in the Symmetry Directions

The dynamical matrix for diamond is a 6×6 Hermitian matrix. In general, it is not possible to factorise it and one has to calculate numerically the six eigenvalues which are the normal mode frequencies in the six branches. In the symmetry directions the dynamical matrix factorises into smaller order matrices and the roots of the secular equation can be written explicitly. Recently experimental dispersion curves in the (100) and (111) directions have been reported⁷². In both these directions the two transverse optic branches as well as the two transverse acoustic branches are degenerate. The solutions are

(a) (100) direction:

$$\left. \begin{array}{l} M \omega_{LO}^2 \\ M \omega_{LA}^2 \end{array} \right\} = 4\alpha + 8\mu (1 - \cos \pi q) \pm 4\alpha \cos(\pi q/2), \quad (36a)$$

$$\left. \begin{array}{l} M \omega_{TO}^2 \\ M \omega_{TA}^2 \end{array} \right\} = 4\alpha + 4(\mu + \lambda) (1 - \cos \pi q) \pm 4 \left[\alpha^2 \cos^2(\pi q/2) + \beta^2 \sin^2(\pi q/2) \right]^{1/2}. \quad (36b)$$

(b) (111) direction:

$$\left. \begin{array}{l} M \omega^2_{LO} \\ M \omega^2_{LA} \end{array} \right\} = 4\alpha + 4(2\mu + \lambda + 2\nu) \sin^2 \pi q \\ \pm 2 \left[\alpha^2 (1 + 3 \cos^2 \pi q) + 4\beta (\beta - \alpha) \sin^2 \pi q \right]^{1/2},$$

(36c)

$$\left. \begin{array}{l} M \omega^2_{TO} \\ M \omega^2_{TA} \end{array} \right\} = 4\alpha + 4(2\mu + \lambda - \nu) \sin^2 \pi q \\ \pm 2 \left[\alpha^2 (1 + 3 \cos^2 \pi q) + \beta (\beta + 2\alpha) \sin^2 \pi q \right]^{1/2}.$$

(36d)

5. Evaluation of the Force Constants

For this purpose, we have four equations relating the five force constants, α , β , λ , μ and ν , to Raman frequency and the three elastic constants C_{11} , C_{12} and C_{44} . These relations have been derived, by the long wave-length limit technique, by Smith⁷³:

$$C_{11} = \frac{1}{2a} (\alpha + 8\mu),$$

$$C_{44} = \frac{1}{2a} \left(\alpha - \frac{\beta^2}{\alpha} + 4\lambda + 4\mu \right), \quad (37)$$

and

$$C_{12} = \frac{1}{2a} (2\beta - \alpha - 4\lambda - 4\mu + 8\nu).$$

The frequency shift of the first order Raman line is obtained by the optical frequency at the origin. This gives

$$\omega_R = \sqrt{8\alpha/m} \quad (38)$$

It may be noted that the force constant δ does not appear in the dispersion relations in the symmetry directions and equations (37) and (38). From (37) and (38), α , λ , μ and ν are expressed in terms of β and substituted in equations (36). The value of β is chosen to fit the experimental curves⁷² at the zone boundaries in the (100) and (111) directions. The elastic constants of diamond have been reported separately by Bhagavantam and Bhimasenachar⁷⁶, Prince and Wooster⁷⁷ and McSkimin and Bond.⁷⁸ The measurements of Prince and Wooster are comparatively imprecise, because the results are deduced from X-ray measurements as against the velocity of sound measurement by the other authors. The three sets of values differ quite a bit from each other, as can be seen from table 5. McSkimin and Bond have discussed in

TABLE 5

Elastic Constants from three different experiments, in dynes/cm²

| | Bhagavantam and Bhimasenachar | Prince and Wooster | McSkimin and Bond |
|----------|-------------------------------------|--------------------------|-------------------------|
| C_{11} | 9.5×10^{12} | 11.0 | 10.76 |
| C_{12} | 3.9 | 3.3 | 1.25 |
| C_{44} | 4.3 | 4.4 | 5.76 |

detail the different sources of error in the experiment. They have mentioned that the error can be as high as 11% in the case of C_{12} due to its small value. The picture regarding the elastic constants appears to be quite obscure. For this reason all the three sets of elastic constants are tried. The value of the Raman frequency is 1332 cm^{-1} ¹¹². It has been found that Bhagavantam and Bhimasenachar's data fits best with the neutron scattering results with the value of β as $.044 \times 10^6 \text{ dynes/cm}^2$. The results of this fit are shown in figure 3. The agreement, in general, is reasonably good. The deviation for the L0, LA and T0 branches in both the symmetry directions is within the experimental error which is 2-3%. For the TA branches, the deviation is maximum at $q/q_m = .3$ ($\sim 10\%$ in the (100) direction and $\sim 18\%$ in the (111) direction) and decreases to less than 1% as $q/q_m \rightarrow 1$. At this stage it may be noted that the two neighbour Born-Von Karman model for germanium⁶⁸ results in a discrepancy of about 66% at the boundary of the TA branch in the (100) direction. No choice of β improves the fit. Even a variation in the value of Raman frequency does not help.

With the elastic data of Bhagavantam and Bhimasenachar and the value of β as $.044 \times 10^6 \text{ dynes/cm}^2$, equations (37) and (38) lead to (in units of 10^6 dynes/cm^2)

$$\alpha = .157, \quad \beta = .044, \quad \lambda = -.0206, \quad \mu = .0226, \quad \nu = .0270 \quad (39)$$

It might be interesting to compare the experimental value of the bulk modulus K with the value obtained by our choice of the

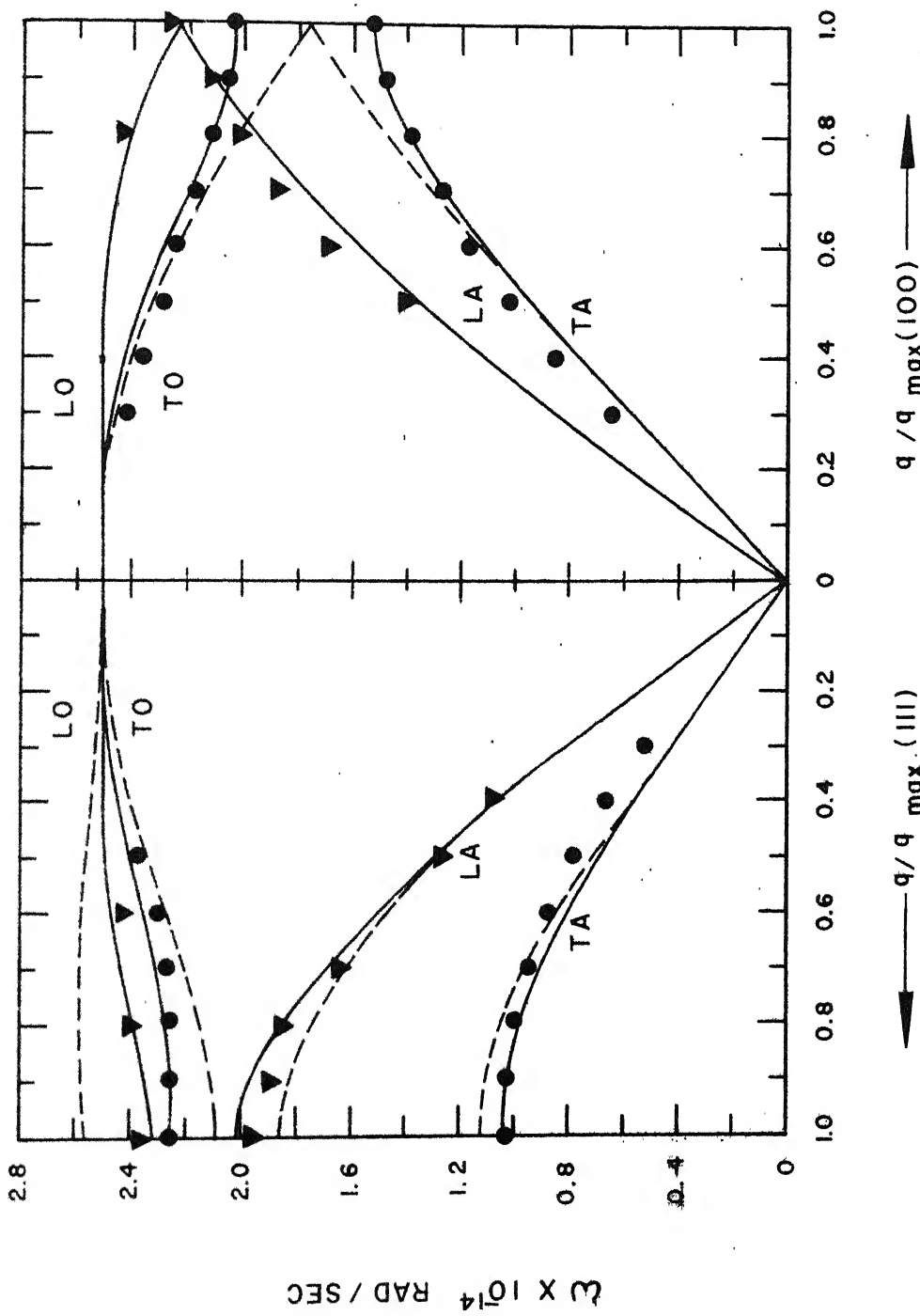


FIG. 3 DISPERSION RELATIONS FOR DIAMOND IN THE SYMMETRY DIRECTIONS. THE CONTINUOUS CURVES AND THE BROKEN CURVES ARE THE CALCULATIONS WITH THE IV AND III SETS OF FORCE CONSTANTS (SEE TABLE 6) RESPECTIVELY. THE CIRCLES AND THE TRIANGLES ARE THE EXPERIMENTAL FREQUENCIES OBTAINED BY WARREN ET AL.

force constants. To calculate K we use the relation:

$$3/K - (c_{11} + c_{12} + c_{44}) = \beta^2 / 2a\alpha, \quad (40)$$

which was suggested by Saint James⁷⁴ on the basis of Laval's theory of elasticity. Using the force constants from (39) and the elastic constants of Bhagavantam and Bhimasenachar, we obtain from (40)

$$K = 0.164 \times 10^{-6} \text{ per megabar,}$$

which agrees very well with Adam's experimental result, $K = 0.16 \times 10^{-6}$ per megabar. However, a different value $K = 0.18 \times 10^{-6}$ per megabar was observed by Williamson⁸¹.

Saint James⁷⁴ chooses the value of β as zero for the following reason. If one uses the mean of the two values of K , Prince and Wooster's data lead to a negative value of β^2/α . This is unphysical since α is unambiguously determined by equation (38) and is positive. Instead, if one uses Adam's value for K , β^2/α is positive and is very small. The value of β can, therefore, be taken to be zero.

Saint James's argument does not seem to be convincing because if one uses, instead of Prince and Wooster's data, the other two data from table 5, β comes out to be sufficiently large ($\sim \alpha/2$). The calculated dispersion curves with the different sets of force constants as calculated by Saint James are found to be in disagreement with the experimental results.

The closest agreement obtained is with Bhagavantam and Bhimasenachar's data and is shown in figure 3.

Determination of δ :

Having obtained the five parameters, we proceed to calculate δ . It, certainly, cannot be obtained by fitting the dispersion relations in the symmetry directions (100) and (111), as it does not occur there at all. δ does occur in the dispersion relations for (110) direction for which no experimental data exists. The only thing one can do is to restrict the nature of the forces. The generalised forces can be thought of as made up of two body forces, three body forces, four body forces and so on. The pair forces are central forces, the triplet forces are the angular forces and the quadruplet forces are the torsional forces. By definition, the angular forces tend to resist deformation of the angle formed by each pair of concurrent bonds and the torsional forces tend to resist deformation of the dihedral angle between each pair of planes determined by the atoms A-B-C and B-C-D respectively, the atoms A-B-C-D being bonded in sequence. We shall assume that the second neighbour forces are made up of central forces, angular forces and torsional forces only. The other kinds of forces for the second neighbours are taken to be negligible. One can show, by deriving the secular equation in a manner explained by de Launey and then comparing the secular equation for the general force model, that

$$\hat{D}_{\text{central}}^9 = \begin{bmatrix} \epsilon & \epsilon & 0 \\ \epsilon & \epsilon & 0 \\ 0 & 0 & 0 \end{bmatrix},$$

$$\hat{D}_{\text{angular}}^9 = \begin{bmatrix} \epsilon' & \epsilon' & 2\epsilon' \\ \epsilon' & \epsilon' & 2\epsilon' \\ -2\epsilon' & -2\epsilon' & -4\epsilon' \end{bmatrix}, \quad (41)$$

$$\hat{D}_{\text{torsional}}^9 = \begin{bmatrix} -\epsilon'' & \epsilon'' & 0 \\ \epsilon'' & -\epsilon'' & 0 \\ 0 & 0 & 0 \end{bmatrix}$$

These individual matrices for the central, angular and torsional forces have also been exhibited by Herman⁶⁸.

Therefore, we obtain for the restricted second neighbour forces,

$$\hat{D}_{\text{general}}^9 = \hat{D}_{\text{central}}^9 + \hat{D}_{\text{angular}}^9 + \hat{D}_{\text{torsional}}^9 \quad (42)$$

From table 4 and equations (41) and (42) we obtain

$$\delta = 2\epsilon' \quad \text{and} \quad \lambda = -4\epsilon',$$

so that

$$\delta = -\lambda/2 \quad (43)$$

Therefore, once we calculate λ , δ is automatically found.

For the sake of comparison, the values of the force constants obtained here along with those calculated by Saint James⁷⁴ and Smith⁷³ are depicted in table 6.

TABLE 6

| Force constants in units of 10^6 dynes/ cm | Calculations of Saint James | | | Values calculated by Smith with constants of Bhagavan- tam | Present calcu- lations IV | | |
|---|--|--------------------------------|---|--|---|--|--|
| | Elastic Constants used are determined by: | | | | | | |
| | Prince and Wooster I | McSkimin and Bond II | Bhagavantam & Bhimasenachar III | | | | |
| α | 0.157 | 0.157 | 0.157 | 0.157 | 0.157 | | |
| β | 0.0 | 0.0 | 0.0 | 0.104 | 0.044 | | |
| λ | -0.0294 | -0.0163 | -0.0236 | 0.0 | -0.0206 | | |
| μ | 0.0293 | 0.0282 | 0.0226 | 0.0226 | 0.0226 | | |
| ν | 0.0343 | 0.0312 | 0.0365 | 0.0226 | 0.0270 | | |
| δ | 0.0122 | 0.0066 | 0.0048 | 0.0 | 0.0103 | | |

It may be mentioned that Smith has considered a similar model except that she restricts the second neighbour forces to only central forces, whereas the present model includes the angular and torsional forces as well. For making the force central she has taken $\lambda = 0$, $\mu = \nu$. For this purpose she ascerts upon the validity of Cauchy relation ($C_{12} = C_{44}$) established by Born who has

shown that in the case of central forces a cubic crystal with centred faces obeys Cauchy's relation. That relation is valid only for a monatomic crystal, where every atom is a centre of symmetry. The supposition of Smith, thus, amounts to neglecting the first neighbours which is unphysical. Though she has used the force constant matrix, D_{central} , given by (41), the arguments used by her are not correct.

Very recently Warren⁸³ has studied a different model for diamond. A negative charge, $-eZ$, situated midway between the neighbouring carbon nuclei is taken to represent the charge density in the bonding direction. The positive charge on the carbon nucleus and the associated spherically symmetric portion of the electron distribution is represented by a positive point charge eZ and a point mass M . Coulomb interactions between the charges and short range interactions extending upto second neighbours are considered. Z^2 is taken as a parameter. Experimental dispersion curves in the (100) direction lead to a negative value of Z^2 , which is clearly unphysical. A least square fit with the TA(111) branch, with the constraint that Z is real, results in $Z = 0$. From this Warren concludes that the charge in the bonds cannot be used to explain the long range nature of forces in covalent crystals. He has also calculated the values of the five parameters, occurring in the dispersion relations in (111) direction for a second neighbour Born-Von Karman model, from the measured frequencies. The values of the parameters so obtained are

$$\alpha = .157, \beta = .0457, \lambda = -.0222, \mu = .0236, \nu = .0255 \quad (44)$$

These values, as can be seen from table 6, are not much different from the present calculations where only one force constant is kept as a parameter.

Frequency distribution functions of diamond with the four sets, I, II, III and IV, of force constants (table 6) will be described in chapter IV. Use has been made of a new method, for the calculation of frequency distribution functions, developed in the next chapter.

CHAPTER III

CALCULATION OF FREQUENCY SPECTRA

1. Introduction

We define the frequency distribution function, $g(\omega)$, of the normal modes of vibrations of crystals such that $g(\omega)d\omega$ is the fraction of frequencies in the interval $(\omega, \omega + d\omega)$. Similarly $G(\omega^2)d\omega^2$ is defined to be the fraction of squared frequencies in the interval $(\omega^2, \omega^2 + d\omega^2)$. The two functions are related by the equation,

$$g(\omega) = 2\omega G(\omega^2). \quad (45)$$

The distribution function is of fundamental importance for the understanding of many properties of crystals (e.g. thermodynamic properties, infrared absorption). It can be experimentally obtained for cubic crystals by using incoherent inelastic scattering of slow neutrons⁸⁴. Unfortunately the number of substances having appreciable incoherent cross-sections is limited and also the energy resolution of these experiments is still too poor to reveal the finer details of $g(\omega)$. Ni, V and Ti are the only crystals for which the measured frequency spectra have been reported so far⁸⁵. In any case the dispersion curves of the normal modes of vibration can be obtained from the data on coherent scattering of slow neutrons and $g(\omega)$ can, in principle, be calculated from these curves. In order to calculate $g(\omega)$, it is essential to

assume a force model and then fit a set of force constants to the dispersion curves and the elastic constants. These force constants give in return the value of the dynamical matrix at every point \underline{q} in the first Brillouin zone. Usually the dispersion curves are measured in high symmetry directions and then analysed by the Born-von Karman theory to obtain the force constants. One might question how adequate the physical description of the dispersion curves is, as given by this model. This is a problem by itself and is irrelevant to the present chapter which is concerned with a new method of computing $g(\omega)$.

The methods for calculating $g(\omega)$ are described at length by Maradudin, Montroll and Weiss⁹. A short review of the various techniques is given here so that the advantages and disadvantages of the new method, that has been developed here, can be seen.

2. Exact Evaluation

One commonly used representation of the distribution function $G(\omega^2)$ is⁸⁶

$$G(\omega^2) = \frac{1}{3sN} \sum_{\underline{k}, j} \delta(\omega^2 - \omega_j^2(\underline{k})), \quad (46)$$

where N is the number of unit cells and s is the number of atoms in the unit cell. The index j is for different branches. The various representations of the δ - function (Dirac δ function)

lead to a number of equivalent formulae relating $G(\omega^2)$ to the dynamical matrix. As an application of formula (46), the case of linear lattices with long range interactions between the atoms can be considered here,

The dispersion relation for a linear chain, with the vibrations in the direction of the chain, is

$$\omega^2(k) = \frac{2}{M} \sum_{n=1} \alpha_n (1 - \cos nk),$$

where α_n is the force constant for the n th neighbour. Three different forms of α_n are assumed: $K \exp(-n\alpha)$, K/n^2 and K/n^4 . We choose the following representation for the delta function:

$$\delta(x) = -\frac{1}{\pi} \lim_{\epsilon \rightarrow 0^+} \text{Im} \frac{1}{x+i\epsilon}. \quad (47)$$

substitution of (47) in (46) leads to

$$\begin{aligned} G(\omega^2) &= -\frac{1}{N\pi} \lim_{\epsilon \rightarrow 0^+} \text{Im} \sum_{k=1}^{2\pi} \frac{1}{\omega^2 + i\epsilon - \omega^2(k)} \\ &= -\frac{1}{2\pi^2} \lim_{\epsilon \rightarrow 0^+} \text{Im} \int_0^{2\pi} \frac{dk}{\omega^2 + i\epsilon - \omega^2(k)} \end{aligned} \quad (48)$$

The integral in equation (48) can easily be calculated for the models we have chosen. $G(X)$ for the three cases is

$$G(X) = \begin{cases} \frac{C}{X^{\frac{1}{2}} (1-X)^{\frac{1}{2}} (1-X \operatorname{sech} \alpha_n / 2)} & \text{, for } \alpha_n = \frac{K}{n} \\ \frac{C}{(1-X)^{\frac{1}{2}}} & \text{, for } \alpha_n = \frac{K}{n^2} \\ \frac{C}{X^{\frac{1}{2}} (1-X^{\frac{1}{2}})^{\frac{1}{2}}} & \text{, for } \alpha_n = \frac{K}{n^4} \end{cases} \quad (49)$$

where $X = \omega^2 / \omega_L^2$, ω_L is the maximum value of the frequency and C is the normalisation constant, so that

$$\int_0^1 G(X) dX = 1. \quad (50)$$

It is evident from (49) that the well known square root singularity in the distribution function in a linear chain persists in the models considered here.

The use of the above method of obtaining closed expressions for the distribution function is limited to very simple cases of linear lattices, where the integral in (48) can be solved exactly. For any reasonably realistic model the dispersion relation, $\omega^2(k)$, is complicated enough so that we have to resort to approximate methods.

3. Approximate Methods

The most straightforward is the root-sampling method, in

which one generates a large number of frequencies by solving the secular equation at a large number of uniformly distributed points in the first Brillouin zone and then sorts these frequencies into suitable ranges (ω , $\omega + \Delta\omega$), so as to produce a histogram representation of $g(\omega)$. The main objection to this method is on the grounds of its being slow, since in order to obtain a reasonably good sampling one needs a very large number of diagonalisations of the dynamical matrix.

Recently, Gilat and Dolling⁸⁸ have introduced the so called "extrapolation method" which considerably accelerates the conventional root sampling method. The idea behind this method is to diagonalise the dynamical matrix $\hat{D}(\underline{q})$ for a relatively small number of evenly spaced points in the reciprocal space and then to find other solutions, for the eigenvalues, in between by means of a Taylor expansion about each such point for each eigenvalue.

The gradient of $\omega(\underline{q})$ needed for this extrapolation is calculated numerically by imposing a small change (δq_i) in the i th component of the wave vector. A new matrix $\hat{\Delta}_{jk}$, representing the change in $\hat{D}(\underline{q})$ is constructed:

$$\hat{\Delta}_{jk} = \hat{D}_{jk}(\underline{q} + \delta q_i) - \hat{D}_{jk}^0(\underline{q}) \quad (50)$$

The change ϵ_j in the j -th eigenvalue is given by perturbation theory:

$$\epsilon_j = \hat{\Delta}'_{jj} + \sum_{k \neq j} \frac{\hat{\Delta}'_{jk}^2}{\hat{\Delta}'_{jj} - \hat{\Delta}'_{kk}}, \quad (51)$$

where $\hat{\Delta}' = \hat{U}^{-1} \hat{\Delta} \hat{U}$ and \hat{U} is the matrix of eigenvectors of $\hat{\Delta}^0$. Hence we obtain

$$(\text{grad}_q \omega_j)_i \approx \frac{\delta \omega_j}{\delta q_i} \approx \frac{1}{2\omega} \frac{\epsilon_j}{\delta q_i} \quad (52)$$

One determines the value of $\omega_j (\underline{q} + \Delta \underline{q})$ from the value of $\omega_j (\underline{q})$ by using $\text{grad}_q \omega_j$ as obtained above, i.e.,

$$\omega_j (\underline{q} + \Delta \underline{q}) = \omega_j (\underline{q}) + \text{grad}_q \omega_j \cdot \Delta \underline{q}. \quad (53)$$

In the actual calculation, the irreducible volume of the first Brillouin zone is divided into a uniform simple cubic mesh of points \underline{q}_c , each point being at the centre of a small cube for which extrapolation is carried out to a finite number of points. Each cube has to be properly weighted according to the symmetry of \underline{q}_c . The main point in this method is that computation of the gradient is much faster than re-diagonalisation. Gilat and Dolling have mentioned that only the first order term on the right hand side of equation (51) need be considered. At the same time it should be noted that for \underline{q} where $\hat{\Delta}^0$ has degenerate

roots, the expression (51) is inapplicable and for such points \hat{D}^0 has to be re-diagonalised to calculate ϵ_j . They have also pointed out that this method leads to relatively less accurate results where the surfaces of constant frequency display rapid variations.

More recently Gilat and Raubenheimer⁸⁹ have extended the extrapolation method for cubic crystals. This involves dividing the irreducible volume of the first Brillouin zone into a cubic mesh and approximating the constant frequency surfaces inside every small cube by a set of parallel planes perpendicular to (ω, q_j, q_c) . The volume element dV falling between two such consecutive planes, describing ω and $\omega + d\omega$, is proportional to the number of frequencies lying between ω and $\omega + d\omega$, and for $d\omega \rightarrow 0$ it can be approximated by

$$dV = S dq, \quad (54)$$

where S is the cross-sectional area of a plane and dq is the thickness of the volume element. The distribution function is given by

$$g(\omega) = \sum_{j, q_c} g(j, q_c; \omega), \quad (55)$$

where the summation is extended over all eigenvalues and cubes. The function $g(j, q_c; \omega)$ gives the distribution of frequencies obtained from $\omega_j(q_c)$ by extrapolating throughout the cube and is given by

$$g(j, \underline{q}_c; \omega) d\omega = C W_{\underline{q}_c} S(\omega) d\omega \text{ for}$$

$$\begin{aligned} \omega_j &= \omega_m \left| \text{grad } \omega_j \right|_{\underline{q}_c} \\ \omega &\leq \omega_j + \omega_m \left| \text{grad } \omega_j \right|_{\underline{q}_c} \\ &= 0 \text{ elsewhere,} \end{aligned} \quad (56)$$

where $W_{\underline{q}_c}$ is a weight factor associated with the symmetry of \underline{q}_c and C is an arbitrary number which is constant throughout the entire Brillouin zone. ω is the distance of any plane from \underline{q}_c and ω_m is the maximum value of ω inside a cube. The frequency ω and the distance ω are related by

$$\omega = \omega_j(\underline{q}_c) \pm \omega \left| \text{grad}_{\underline{q}} \omega_j \right|_{\underline{q} = \underline{q}_c} \quad (57)$$

Gilat and Raubenheimer have given the expression for the cross-section area, in terms of the direction cosines of the gradient and the distance ω . In this method the entire Brillouin zone and not just a finite number of selected points contributes to $g(\omega)$ and this is precisely the advantage it has over the extrapolation method. The errors, due to degeneracies and due to neglecting higher order contributions to the gradient, that occur in the extrapolation method persist. There are additional errors due to the assumption that constant frequency surfaces are parallel planes within the cube.

Another method which has had some popularity is the moment method. This involves expansion of $g(\omega)$ in a series of Legendre polynomials in which the coefficients of the successive

terms are linear combinations of the moments of the dynamical matrix. $g(\omega)$ is written as

$$g(\omega) = \sum_{n=0}^{\infty} a_n P_n(\omega/\omega_L) , \quad (58)$$

where ω_L is the maximum frequency and

$$a_n = \frac{(2n+1)}{2} \int_{-1}^1 g(\omega_L x) P_n(x) dx . \quad (59)$$

Since $g(\omega)$ is an even function of ω , only the even coefficients, a_{2n} , are nonvanishing. Therefore we have

$$a_{2n} = \frac{(4n+1)}{\omega_L} \int_{-1}^1 g(x) P_{2n}(x) dx \\ = \left(\frac{4n+1}{\omega_L} \right) \left| P_{2n}(x) \right|_{x=U_{2n}} , \quad (60)$$

where U_{2n} is related to the $2n$ -th moment (μ_{2n}) :

$$U_{2n} = \frac{\mu_{2n}}{\omega_L^{2n}} , \quad \mu_{2n} = \frac{1}{3sN} \sum_k T_r D^k(k) . \quad (61)$$

The moment method has been applied by Montroll and collaborators⁹⁰⁻⁹² to the evaluation of frequency spectra of a two dimensional square lattice and of simple and body-centred

cubic lattices. The chief advantage of this method over the root sampling methods is that one gets an analytic expression for $g(\omega)$. One of the major deficiencies is that it is inaccurate in the vicinity of a singularity due to slow convergence of the Legendre polynomial expansion.

An improved method due independently to Lax and Lebowitz⁹³ and to Rosonstock⁹⁴ takes into account the presence of singularities. This method assumes that it is possible to find the singular part, $g_S(x)$, of the distribution function. $g_S(x)$ is subtracted from $g(x)$ and the remainder is approximated by a linear combination of n Legendre polynomials. The first $n-2$ coefficients of the expansion are determined by requiring that the first $n-2$ moments of the approximate function agree with the exact ones. The remaining two coefficients are fixed by the value of the distribution function at the end points. This method is very efficient in the sense that only a few moments yield quite an accurate behaviour of the distribution function. Despite the great amount of work on the location of critical points, in particular by Van Hove⁹⁵, Rosonstock⁹⁶ and Phillips⁹⁷, no general scheme has been found that will ensure that all the critical points have been found. The application of this method, therefore, is restricted to analytic models as one requires the knowledge of location and shapes of singularities.

O. Isenberg⁹⁸ has introduced a new method for the calculation of a large number of moments for crystals with short-

range interactions. He has proved a theorem that states:

If $\mu_{2n}(N)$ is the $2n$ -th moment of the spectrum for a finite lattice, with cyclic boundary conditions, in which the interactions extend to T neighbours, then

$$\mu_{2n}(N) = \mu_{2n}(\infty), \text{ provided } n < N/T \quad (62)$$

where N^3 is the number of atoms in the finite lattice. The use of the theorem along with the relations⁹⁹

$$S_1 + p_1 = 0$$

-----.

$$S_j + p_1 S_{j-1} + p_2 S_{j-2} + \dots + p_j S_{j-j} = 0$$

-----.

$$S_n + p_1 S_{n-1} + p_2 S_{n-2} + \dots + p_j S_{n-j} = 0,$$

for $n > j$

(63)

saves the labour of calculating moments considerably. Here S_n is the n th trace of the $j \times j$ dynamical matrix for a point in the first Brillouin zone and p_j 's are the unknowns that can be determined from the first j equations. The calculation consists in evaluating the first j traces for a point in the Brillouin zone. The subsequent traces are obtained from equations (63). This is repeated for all the allowed wave-vectors. The corresponding values of S 's are summed up, after suitably weighting them according to the position of the point in the zone, to give us finally the first n even moments on the finite

lattice and hence on the infinite lattice because of equation (62).

Mention may also be made of Houston's method which has enjoyed some popularity because of providing very good results at low frequencies. This method uses expansion of the function $g_j(\omega, \theta, \varphi)$, the distribution function per unit solid angle for the j th branch, in terms of Kubic harmonics,

$$g_j(\omega, \theta, \varphi) = \sum_{m=0}^{\infty} a_m(\omega) K_m(\theta, \varphi), \quad (64)$$

where prime on the summation sign indicates the omission of the term corresponding to $m = 1$. Now along the symmetry directions the secular equation can be solved analytically for $\omega = \omega_j(k; \theta, \varphi)$ and for simple enough models this equation can be inverted to obtain k and hence $g_j(\omega, \theta, \varphi)$ which is simply $(1/3 \cdot sV) k_j^2(\omega, \theta, \varphi) dK_j(\omega, \theta, \varphi)/d\omega$. The number of terms that we should retain in (64) is determined by the number of directions along which $g_j(\omega, \theta, \varphi)$ can be obtained in an exact manner. The coefficients $a_m(\omega)$ are evaluated by solving a set of simultaneous equations. The total spectrum is then given by

$$g_j(\omega) = \int_0^{\pi} \sin \theta d\theta \int_0^{2\pi} g_j(\omega, \theta, \varphi) d\varphi. \quad (65)$$

Houston's method has a serious drawback of introducing spurious square root singularities into the spectrum. Moreover, the derived frequency spectrum will converge to the actual one only if $g_j(\omega, \theta, \varphi)$ is evaluated along a very large number of directions. This itself indicates the impracticability of the method.

Hwang¹⁰¹ has suggested interpolation between symmetry lines or planes to obtain frequency contours within the Brillouin zone. The rest of the procedure is same as in Houston's method. The only calculation carried out by Hwang was for the two dimensional Bowers-Rosenstock model. This method when combined with an exact handling of singularities gave excellent agreement with the exact spectrum.

Still another method that requires the use of contours of constant frequency is due to Hwang and Wang¹⁰². A few important contours of constant frequency on the surface of the Brillouin zone are calculated. The contours on the inner planes are traced by an interpolation scheme. The volume enclosed by the surface of constant frequency is computed by numerical integration and fitted in a form

$$V(\omega^2) = \sum_i a_i (\omega^2 - c_i)^{3/2} + \sum_n b_n \omega^{2n}, \quad (66)$$

where the first term is put according to result of singularity analysis^{95,96}. Finally $G(\omega^2)$ is obtained on differentiating $V(\omega^2)$ with respect to ω^2 . This method was applied to the two dimensional and three dimensional simple cubic lattices and an excellent agreement with the exact frequency distribution was obtained.

In short, these methods can be classified into two main groups, the sampling methods and methods involving series expansions. The sampling methods enable a histogram approximation of the frequency spectrum. The advent of digital computers has led many workers to carry out extensive sampling calculations. The accuracy

is greatly improved due to modifications by Gilat and Dolling, and Gilat and Raubenheimer. These methods require the spectrum to be stored numerically in the form of a histogram. Therefore numerical techniques have to be applied to obtain the thermodynamic properties, and the accuracy of the final result is not easy to assess. This makes it difficult to compare related models. Among the series expansions, Houston's modified methods, due to Hwang, and Hwang and Wang, have the disadvantage of requiring the knowledge of critical points and the constant frequency contours which are difficult to obtain even on the faces of the Brillouin zone, except for very simple models. The moment method, as such, is slow due to the poor convergence of the Legendre polynomials, and though the convergence can be improved in a manner suggested by Lax and Lebowitz, the computation problems associated with improving the convergence are formidable because of the need to know the location of critical points. Isenberg's method permits us to calculate a large number of moments on lattices where only short range interactions are present. A new series expansion method is suggested in the following.

4. The Fourier Series Expansion Method¹⁰⁹

The present method involves the use of sine functions as the basis functions for the expansion of the distribution function. Perhaps the only reason Legendre polynomials have been used traditionally is because the coefficients of expansion can be evaluated in terms of moments. The use of other orthonormal sets, such as sine functions, does not offer this advantage. However, this difficulty is a minor one in the age of high speed computers.

There are natural reasons for the choice of sine functions.

The distribution function of a three dimensional lattice is zero at the end points and is usually continuous in between, its only peculiarities being some kinks leading to discontinuities in the derivative. The Fourier series of such a function is highly convergent⁹ and therefore leads to a more accurate and convenient representation. As in the case of the Legendre polynomial representation, the Fourier series representation of the distribution function provides a means of obtaining a series expansion of any additive function of the normal mode frequencies of the lattice, such as thermodynamic properties.

We shall consider here the distribution function $G(X)$ of the quantity $X = \omega^2 / \omega_{\max}^2$ in one of the branches. The results can be extended to other branches in the acoustic and optical bands in an obvious manner. The dispersion relation for the branch under consideration can be written as

$$X = X(\underline{k}), \quad (67)$$

where $X(\underline{k})$ gives the functional dependence of X on the wave vector \underline{k} .

The distribution function can be expanded in a Fourier series in the form

$$G(X) = \sum_{n=0}^{\infty} A_n \sin(n \pi X), \quad (68)$$

so that

$$\begin{aligned}
 A_n &= 2 \int_0^1 G(X) \sin(n\pi X) dX \\
 &= 2/V^* \int_{V^*} \sin(n\pi X(\underline{k})) d^3 \underline{k}, \tag{69}
 \end{aligned}$$

where V^* is the volume of the first Brillouin zone.

The evaluation of the coefficients A_n thus amounts to solving the integral in equation (69) using the explicit form of the dispersion relation in equation (67). For some simple models the integral can be done analytically, but, however, it can be evaluated numerically for all models. Equation (69) when substituted in equation (68) leads to the required representation for $G(X)$.

5. Applications

The method described above is applied to calculate $G(X)$ for a model where the integral for A_n can be evaluated analytically. We consider here a m -dimensional simple cubic lattice with nearest neighbour central and non-central force constants being equal and each atom having only one degree of freedom¹⁰⁴. The dispersion relation in this case can be written as

$$X(\underline{k}) = 1/2m (m - \cos k_1 - \cos k_2 - \dots - \cos k_m), \tag{70}$$

where k_i is the i th component of the m -dimensional vector \underline{k} .

Substituting (70) in (69) and noting that $V^* = (2\pi)^m$, we have,

$$A_n = 2/(2\pi)^m \iint_0^{2\pi} \dots \int \sin \left[n\pi/2m (m - \cos k_1 - \cos k_2 - \dots - \cos k_m) \right] dk_1 dk_2 \dots dk_m \tag{71}$$

After expanding out the integrand it can easily be seen that the integral vanishes for even values of n . The nonvanishing coefficients are,

$$\begin{aligned} A_{2n+1} &= 2(-1)^n \prod_{j=1}^m \left[\frac{1}{2\pi} \int_0^{2\pi} \cos \left(\frac{2n+1}{2m} \pi \cos k_j \right) dk_j \right] \\ &= 2(-1)^n \left[J_0 \left(\frac{2n+1}{2m} \pi \right) \right]^m. \end{aligned} \quad (72)$$

The normalised form of $G(X)$ is given by,

$$G_m(X) = \frac{\sum_{n=0}^{\infty} (-1)^n \left[J_0 \left(\frac{2n+1}{2m} \pi \right) \right]^m \sin((2n+1)\pi X)}{\sum_{n=0}^{\infty} (-1)^n \frac{2}{\pi(2n+1)} \left[J_0 \left(\frac{2n+1}{2m} \pi \right) \right]^m}. \quad (73)$$

For the one and two dimensional cases, i.e., for $m = 1$ and 2, the convergence of the series in equation (73) is bound to be poor due to the occurrence of infinities in $G(X)$. Even with 30 terms in the series, the approximate distribution function for the one dimensional case was found to oscillate about the curve obtained by exact calculation. The oscillations in $G(X)$ are due to strong infinities at the ends.

In the two dimensional case table 7 depicts the approximate $G(X)$ with 30 terms in the series, along with the exact one calculated by Montroll¹⁰⁴. The agreement is surprisingly good, except at $X = 0.5$ and $X = 0$ and 1, considering the fact that no attempt has been made to handle the logarithmic singularity at $X = 0.5$ and non-zero values of $G(X)$ at $X = 0$ and 1 in the manner suggested by Lax and Lebowitz. The present method gives a sharp peak in place of the

logarithmic infinity at $X = .5$.

TABLE 7

| X | $G_2(X)$ | Exact | Computed |
|-----|----------|--------|----------|
| 0 | | .6366 | 0 |
| .05 | | .6706 | .7117 |
| .10 | | .7096 | .6988 |
| .15 | | .7549 | .7608 |
| .20 | | .8086 | .8160 |
| .25 | | .8740 | .8685 |
| .30 | | .9560 | .9730 |
| .35 | | 1.0650 | 1.0537 |
| .40 | | 1.2224 | 1.2445 |
| .45 | | 1.4977 | 1.4887 |
| .50 | ∞ | | 2.6689 |

The height of this peak is expected to increase with increase in the number of terms in the series. It may be noted that equation(68) would always lead to zero values of $G(X)$ at the end points. While this is unrealistic for the two dimensional case, it is possible to extrapolate to $X = 0$ and 1 from the neighbouring points to get values close to the true ones. It will be shown later that one can get a very satisfactory representation for $G(X)$ of a lamellar crystal by modifying this method in the manner suggested by Lax and Lebowitz.⁹³

In the three dimensional case approximate $G(X)$, taking

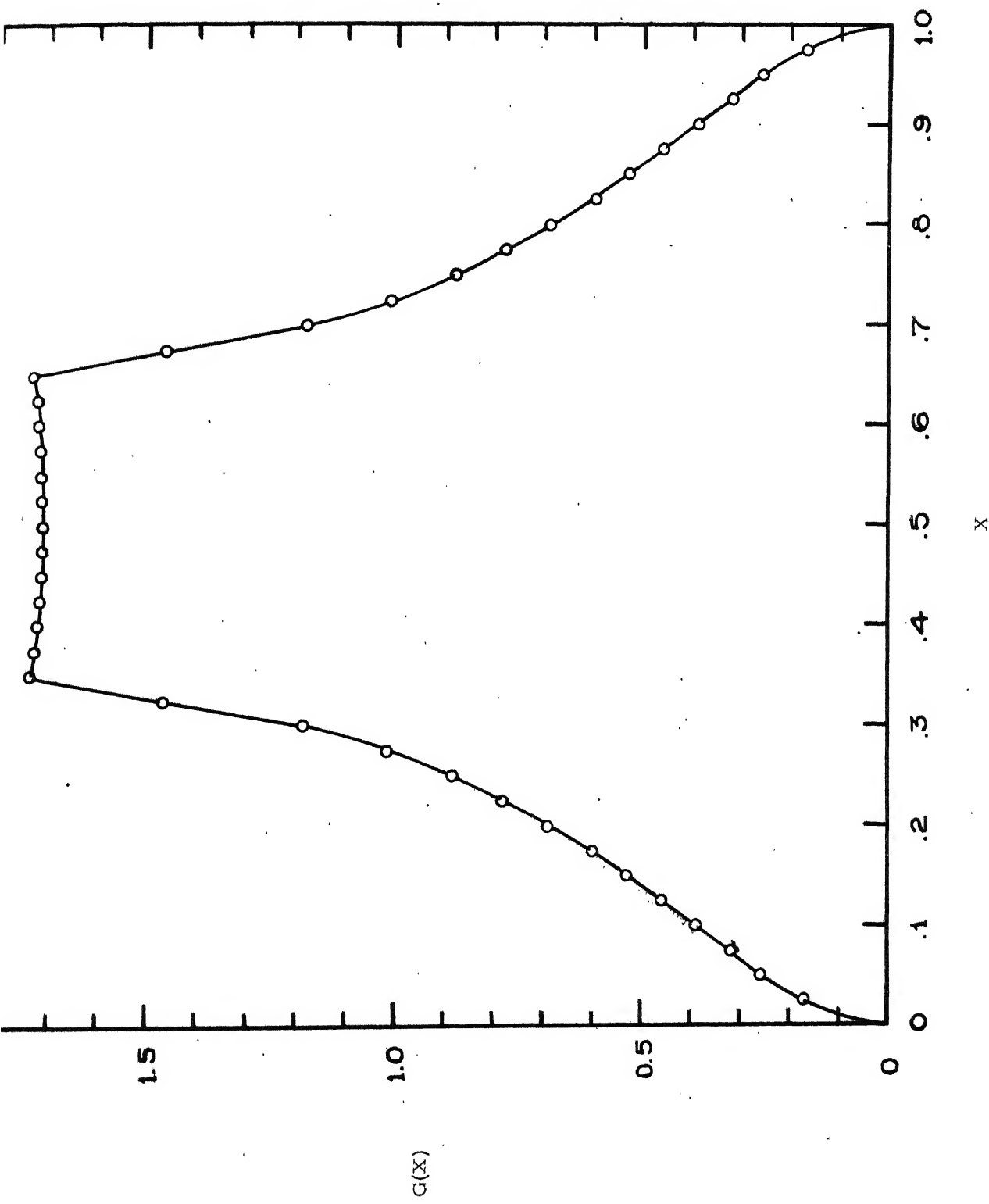


FIG. 4 FREQUENCY SPECTRUM OF A 3-D SIMPLE CUBIC LATTICE (SCALAR MODEL). HERE $X = \omega^2/\omega_L^2$

15, 30 and 40 terms, along with the one obtained by taking 80 terms in the series (which can be considered to be the exact one) is depicted in Table 8, for getting an idea of the convergence of the series. Figure 4 shows a plot of $G_3(X)$ as obtained by Bowers and Rosenstock⁸⁶ and Montroll¹⁰⁴. The points are the results of the Fourier expansion method with 30 terms in the series. With 15 terms, $G(X)$ agrees with the exact one within 1% except near the end points and the critical point at $X = 1/3$ where the error is 4-5%. Increasing the number of terms to 30 and 40 decreases the error but the agreement at the end points does not improve much. This is due to the inability of the Fourier series to reproduce $X^{1/2}$ behaviour of $G(X)$ when $X \rightarrow 0$. In the following we shall see how this difficulty can be overcome when low temperature studies are made.

6. A Modified Functional Expansion Method

For the one and two dimensional lattices the Fourier series expansion method leads to incorrect results. In the two dimensional case, however, $G(X)$ obtained by this method agrees closely with the exact one over most of the region, so that in those cases where the finer details of $G(X)$ are unimportant, such as the calculation of the thermodynamic properties, $G(X)$ computed by the above method can be used. To obtain a more exact form of $G(X)$ one can include cosine functions in the series expansion to give nonvanishing values at the end points, and a suitable number of singular functions to reproduce the desired singularities. For the purpose of illustration, we have chosen a graphite-type laminar hexagonal lattice with nearest

TABLE 8

Frequency distribution function of a three dimensional simple cubic lattice.

| X | Exact $G_3(X)$ | Computed 15 terms | $G_3(X)$ with 30 terms | with 40 terms |
|-------|-------------------|----------------------|---------------------------|------------------|
| 0 | 0 | 0 | 0 | 0 |
| 0.025 | 0.175 | 0.183 | 0.171 | 0.169 |
| 0.050 | 0.254 | 0.248 | 0.257 | 0.252 |
| 0.075 | 0.326 | 0.329 | 0.328 | 0.324 |
| 0.100 | 0.393 | 0.392 | 0.393 | 0.392 |
| 0.125 | 0.460 | 0.458 | 0.458 | 0.460 |
| 0.150 | 0.532 | 0.537 | 0.530 | 0.530 |
| 0.175 | 0.605 | 0.598 | 0.608 | 0.605 |
| 0.200 | 0.689 | 0.696 | 0.691 | 0.687 |
| 0.225 | 0.778 | 0.774 | 0.779 | 0.778 |
| 0.250 | 0.887 | 0.887 | 0.881 | 0.884 |
| 0.275 | 1.011 | 1.019 | 1.011 | 1.013 |
| 0.300 | 1.183 | 1.162 | 1.188 | 1.181 |
| 0.325 | 1.446 | 1.500 | 1.479 | 1.464 |
| 0.350 | 1.727 | 1.745 | 1.745 | 1.731 |
| 0.375 | 1.727 | 1.725 | 1.731 | 1.723 |
| 0.400 | 1.720 | 1.718 | 1.720 | 1.718 |
| 0.425 | 1.717 | 1.722 | 1.715 | 1.715 |
| 0.450 | 1.715 | 1.711 | 1.714 | 1.712 |
| 0.475 | 1.712 | 1.717 | 1.714 | 1.711 |
| 0.500 | 1.713 | 1.710 | 1.714 | 1.710 |

neighbour interactions. The dispersion relations¹⁰⁵ for this model are

$$X = 1/2 \pm 1/6 \left[4 \cos \Theta (\cos \Theta + \cos \varphi) + 1 \right]^{1/2}, \quad (74)$$

where Θ and φ are proportional to the rectangular components of the wave vector in reciprocal space and range from 0 to π . The positive and negative signs correspond to the two branches. $G(X)$ has been evaluated in a closed form by several authors (see e.g. ref. 105). It is

$$\begin{aligned} G(X) &= \frac{9(1-2X)}{\pi^2 B} K(A/B) \quad \text{for } 0 \leq X \leq 1/3 \\ &= \frac{9(1-2X)}{\pi^2 A} K(B/A) \quad \text{for } 1/3 \leq X \leq 1/2 \end{aligned} \quad (75)$$

$$\begin{aligned} \text{and } G(X) &= G(1-X) \quad \text{for } 1/2 \leq X \leq 1 \\ &= 0 \quad \text{for } X < 0 \text{ or } X > 1, \end{aligned}$$

where

$$A^2 = 3X(2-3X)^3, \quad B^2 = 3(1-2X)$$

and

$$K(z) = \int_0^{\pi/2} (1-z^2 \sin^2 \xi)^{-1/2} d\xi.$$

$G(X)$ contains logarithmic singularities at $X = 1/3$ and $X = 2/3$.

To obtain the distribution function by the modified Fourier expansion method, we have included two extra terms, $B_1 \cos \pi f$ and $B_2 \ln |f - 2/3|$, the former to give a nonzero value at the origin and the latter to reproduce the singularity at the point

$f = 2/3$, where f is ω^2/ω_{\max}^2 for the acoustic branch and is $2X$.

The distribution function for this branch is

$$G(f) = B_1 \cos \pi f + B_2 \ln |f - 2/3| + \sum_{n=1}^p A_n \sin n \pi f \quad (76)$$

It may be mentioned that a prior knowledge of B_1 and B_2 is not needed. A_n , B_1 and B_2 are calculated by solving $p + 2$ simultaneous linear equations. It has been found, by trying successively increasing values of p , that only seven sine functions are sufficient to yield a satisfactory agreement with the correct $G(X)$ given by equations (75). The computed values of the coefficients are

$$\begin{aligned} B_1 &= .302, & B_2 &= - .275, & A_1 &= 8.275 \times 10^{-2}, \\ A_2 &= -1.909 \times 10^{-2}, & A_3 &= -1.680 \times 10^{-2}, & A_4 &= -1.928 \times 10^{-2}, \\ A_5 &= 1.962 \times 10^{-2}, & A_6 &= -8.772 \times 10^{-3}, & A_7 &= -6.530 \times 10^{-3}. \end{aligned}$$

The distribution function for the other branch can be obtained by reflexion of $G(f)$ given by equation (76) about $f = 1.0$ axis for this model. In figure 5, the solid curve is the exact result from equations (75) and the points represent the values obtained by this modified method.

In exactly the same manner, in the three dimensional models a better agreement between the approximate $G(X)$, and the exact one, at the end points, can be achieved. The behaviour of $G(X)$ at the end points is known to be¹⁰⁴

$$G(X) \propto X^{1/2} \quad \text{for } X \rightarrow 0 \quad (77)$$

$$\propto (1 - X)^{1/2} \quad \text{for } X \rightarrow 1$$

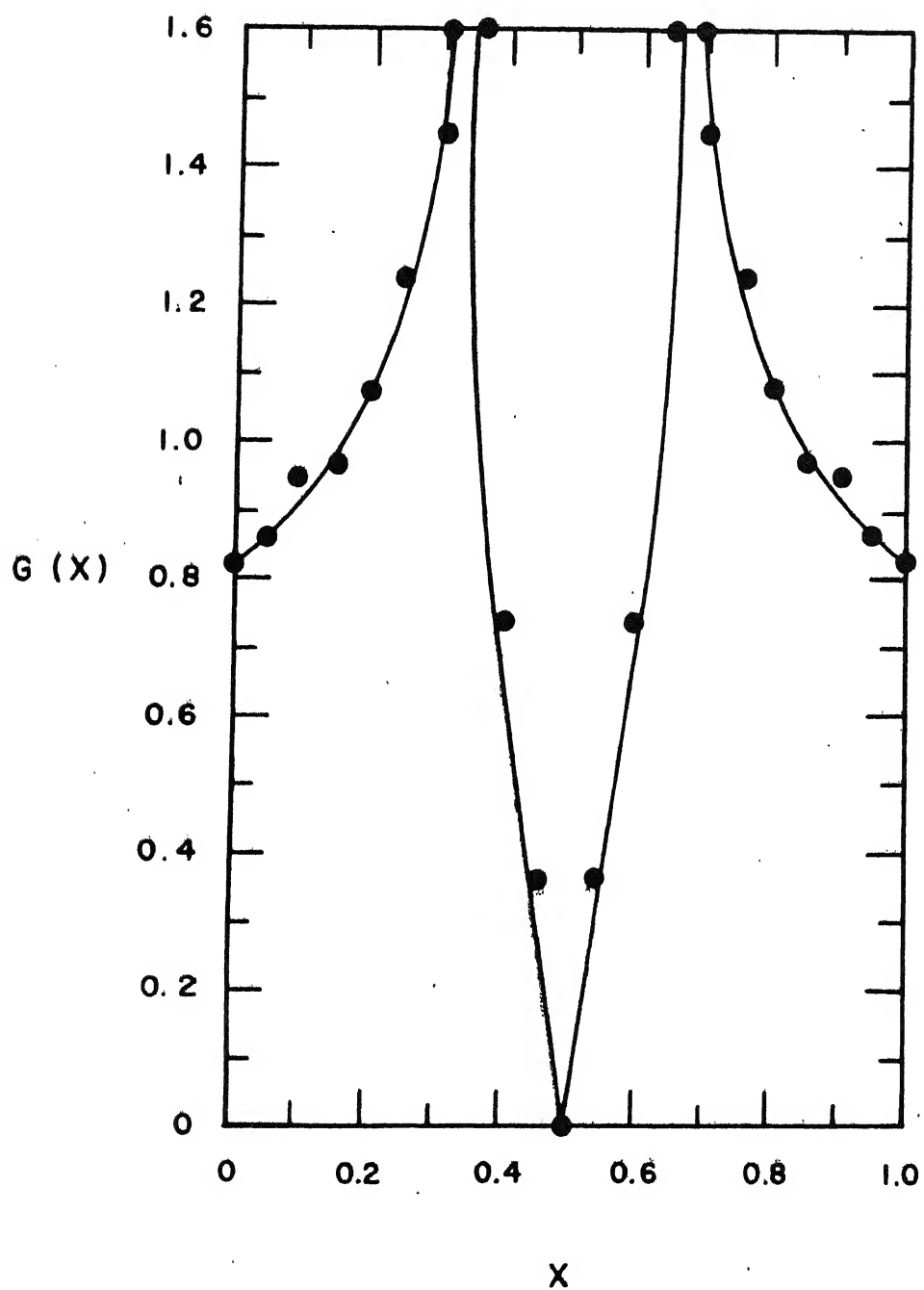


FIG. 5 $G(X)$ FOR A GRAPHITE - TYPE TWO DIMENSIONAL LATTICE WITH NEAREST NEIGHBOUR CENTRAL FORCE INTERACTION. THE SOLID CURVE REPRESENTS THE EXACT CALCULATION DUE TO ROSENSTOCK, AND THE CIRCLES SHOW THE RESULTS OBTAINED BY THE PRESENT METHOD.

Now if we introduce a term $X^{1/2} (1 - X)^{1/2}$ in the series expansion, $G(X)$ will still vanish at the end points but will behave in the neighbourhood as required by (77).

7. The Distribution Function for some F.C.C. and B.C.C. Lattice Models

We proceed to apply the unmodified Fourier series expansion method to compute the distribution functions of some f.c.c. and b.c.c. lattice models, the modification being not necessary as shall be pointed out in the next section. For f.c.c. lattices we assume a central force model. For b.c.c. lattices we take a model in which each atom interacts with its nearest neighbour through central and angular forces and with its next nearest neighbours through central forces. For both types of lattices the interactions have been limited upto second neighbours. The secular equations can be written as follows:

(a) F.C.C. lattice

$$\begin{vmatrix} 2 - c_1(c_2 + c_3) + 2\sigma s_1^2 - \lambda^2 & s_1 s_2 & s_1 s_3 \\ s_1 s_2 & 2 - c_2(c_1 + c_3) + 2\sigma s_2^2 - \lambda^2 & s_2 s_3 \\ s_1 s_3 & s_2 s_3 & 2 - c_3(c_1 + c_2) + 2\sigma s_3^2 - \lambda^2 \end{vmatrix} = 0. \quad (78)$$

(b) B.C.C. Lattice

$$\begin{vmatrix}
 (1+2\beta)(1-c_1c_2c_3) & (1-\beta)s_1s_2c_3 & (1-\beta)s_1c_2s_3 \\
 +\frac{3}{2}\sigma s_1^2 - \lambda^2 & & \\
 \\
 (1-\beta)s_1s_2c_3 & (1+2\beta)(1-c_1c_2c_3) & (1-\beta)s_2s_3c_1 \\
 +\frac{3}{2}\sigma s_2^2 - \lambda^2 & & \\
 \\
 (1-\beta)s_1c_2s_3 & (1-\beta)s_2s_3c_1 & (1+2\beta)(1-c_1c_2c_3) \\
 +\frac{3}{2}\sigma s_3^2 - \lambda^2 & & \\
 \end{vmatrix} = 0, \quad (79)$$

where $c_j = \cos k_j$, $s_j = \sin k_j$, $k_j = q_j a$, $2a$ = lattice constant

and $\lambda^2 = \begin{cases} M\omega^2/2\alpha, & \text{for F.C.C. lattice} \\ 3M\omega^2/8\alpha, & \text{for B.C.C. lattice.} \end{cases}$

Here M is the mass of the atom in the lattice. β and σ are the nearest neighbour noncentral and next-nearest neighbour central force constants expressed in units of the nearest neighbour central force constant α . q_j is the j th rectangular component of the wave vector \underline{q} .

Solving the cubic equation for λ^2 we get the dispersion relation for each frequency branch. For each branch $G(X)$ can be evaluated by using equations (68) and (69), taking care to

ensure that the integration in equation (69) is done through the Brillouin zone corresponding to the lattice model. In these cubic lattices, the symmetry of the constant frequency surfaces can be exploited by doing the integration through only 1/48 of the first Brillouin zone, which in the F.C.C. lattice is the part of the zone enclosed in the trihedral angle defined by (001), (101) and (111) directions, and in the B.C.C. case is the part enclosed within the tetrahedron bounded by the planes $k_2 = 0$, $k_1 + k_3 = \pi$, $k_1 = k_2$ and $k_1 = k_3$, with their ranges defined by

$$0 \leq k_1, k_2 \leq \pi/2, \text{ and } 0 \leq k_3 \leq \pi.$$

The integration required in equation (69) was carried out by a CDC-3600 electronic computer. For the F.C.C. lattice we have used the procedure given by Overton and Dent¹⁰⁶ to evaluate the frequencies in a particular branch in the region of integration. For the B.C.C. lattice the volume integral is expressed as a sum of two three dimensional integrals:

$$\int_{V^*} \sin [n \pi \mathbf{x}(\underline{k})] d^3 \underline{k} = \int_0^{\pi/2} dk_3 \int_0^{k_3} dk_1 \int_0^{k_1} \sin [n \pi \mathbf{x}(\underline{k})] dk_2 + \int_{\pi/2}^{\pi} dk_3 \int_0^{\pi-k_3} dk_1 \int_0^{k_1} \sin [n \pi \mathbf{x}(\underline{k})] dk_2 \quad (80)$$

Both the integrals on the right hand side of (80) are written in the same program, with the machine instructed to change the upper limit of the variable k_1 , from k_3 to $\pi - k_3$, as soon as the value of k_3 exceeds $\pi/2$. For the purpose of integration the whole volume of the irreducible part of the zone is divided into cubes of edge length $\pi/100$ along each axis. Thus by increasing k_3 , k_1 and k_2 in steps of $\pi/100$ upto their respective maximum limits, the machine calculates the value of the integrand at the centre of each cube and adds them by storing them at the same location. The final result is obtained by multiplying it with the volume of the cube $(\pi/100)^3$.

We have calculated the first fifteen coefficients A_n of the function $\sin(n\pi x)$ in equation (68) for eleven values of σ ranging from -.25 to +.25 in steps of .05, for the face-centred cubic lattices and five values of β , from $-\sigma/5$ to $+\sigma/5$ in steps of $\sigma/10$, corresponding to each of the eleven values of σ , from 0 to 1 in steps of .1, for the body-centred cubic lattices. Table 9 contains these coefficients for three values of σ for the face-centred lattices. Tables 10(a) and 10(b) contain the coefficients for three values of β with $\sigma = 0$ and three values of σ with $\beta = 0$, respectively for the body-centred cubic lattices. Here L , T_1 and T_2 refer to the longitudinal and two transverse branches respectively. The dimensionless variable X is the ratio $\lambda^2 / \lambda_{\max}^2$, so that the range of X is from zero to one for each branch. The coefficients have been so normalised that the area enclosed by $G(X)$ for each branch is one, when $G(X)$

TABLE 9
Face - centred cubic lattice

| n | $\sigma = -0.1$ | | | $\sigma = 0$ | | | $\sigma = 0.1$ | | |
|----|-----------------|--------|--------|--------------|--------|--------|----------------|--------|--------|
| | L | T_1 | T_2 | L | T_1 | T_2 | L | T_1 | T_2 |
| 1 | 1.146 | 1.675 | 1.473 | 1.051 | 1.723 | 1.558 | 1.123 | 1.734 | 1.612 |
| 2 | -1.172 | 0.913 | 1.118 | -1.142 | 0.704 | 1.110 | -1.256 | 0.682 | 1.168 |
| 3 | 1.112 | -0.407 | 0.234 | 1.147 | -0.612 | 0.094 | 1.217 | -0.680 | -0.052 |
| 4 | -0.886 | -0.262 | 0.138 | -0.982 | -0.161 | -0.134 | -0.934 | -0.177 | -0.440 |
| 5 | 0.574 | 0.211 | 0.106 | 0.751 | 0.314 | -0.199 | 0.551 | 0.381 | -0.298 |
| 6 | -0.229 | 0.005 | -0.170 | -0.446 | -0.060 | -0.197 | -0.118 | -0.035 | -0.012 |
| 7 | -0.068 | -0.142 | -0.118 | 0.156 | -0.146 | 0.102 | -0.227 | -0.170 | 0.295 |
| 8 | 0.309 | 0.002 | 0.046 | 0.104 | 0.091 | 0.143 | 0.443 | 0.120 | 0.168 |
| 9 | -0.435 | 0.015 | 0.008 | -0.276 | 0.075 | -0.002 | -0.478 | 0.095 | -0.111 |
| 10 | 0.460 | 0.017 | 0.089 | 0.364 | 0.025 | 0.128 | 0.373 | -0.029 | 0.025 |
| 11 | -0.378 | 0.097 | 0.173 | -0.350 | 0.024 | 0.098 | -0.168 | -0.011 | 0.087 |
| 12 | 0.236 | 0.037 | -0.029 | 0.266 | -0.053 | -0.173 | -0.046 | -0.040 | -0.185 |
| 13 | -0.057 | -0.034 | -0.099 | -0.126 | -0.023 | -0.071 | 0.216 | -0.007 | -0.102 |
| 14 | -0.103 | 0.016 | 0.120 | -0.021 | 0.046 | 0.144 | -0.289 | 0.081 | 0.229 |
| 15 | 0.225 | 0.013 | 0.110 | 0.157 | -0.016 | -0.016 | 0.269 | 0.005 | 0.104 |

L refers to the longitudinal branch, and T_1 and T_2 to the transverse branches.

TABLE 10(a)

Body-centred cubic lattice, $\sigma = 0$

| | $\beta = -0.05$ | | | $\beta = 0$ | | | $\beta = 0.05$ | | |
|-----|-----------------|-------|--------|-------------|-------|--------|----------------|-------|--------|
| n | L | T_1 | T_2 | L | T_1 | T_2 | L | T_1 | T_2 |
| 1 | 1.081 | 1.072 | 1.703 | 1.066 | 1.075 | 1.703 | 1.056 | 1.082 | 1.702 |
| 2 | -0.994 | 0.940 | 0.153 | -0.990 | 0.945 | 0.150 | -0.988 | 0.952 | 0.147 |
| 3 | 0.925 | 0.839 | -0.614 | 0.921 | 0.840 | -0.616 | 0.919 | 0.841 | -0.617 |
| 4 | -0.718 | 0.619 | -0.070 | -0.717 | 0.616 | -0.070 | -0.714 | 0.611 | -0.068 |
| 5 | 0.546 | 0.502 | 0.519 | 0.544 | 0.495 | 0.515 | 0.541 | 0.486 | 0.519 |
| 6 | -0.361 | 0.401 | 0.079 | -0.365 | 0.393 | 0.076 | +0.365 | 0.382 | 0.074 |
| 7 | 0.242 | 0.368 | -0.347 | 0.253 | 0.358 | -0.349 | 0.260 | 0.346 | -0.350 |
| 8 | -0.141 | 0.306 | -0.070 | -0.164 | 0.296 | -0.070 | -0.181 | 0.283 | -0.068 |
| 9 | 0.100 | 0.265 | 0.317 | 0.134 | 0.253 | 0.318 | 0.161 | 0.240 | 0.319 |
| 10 | -0.079 | 0.207 | 0.070 | -0.124 | 0.197 | 0.068 | -0.160 | 0.184 | 0.067 |
| 11 | 0.095 | 0.183 | -0.234 | 0.146 | 0.175 | -0.236 | 0.186 | 0.164 | -0.238 |
| 12 | -0.107 | 0.155 | -0.058 | -0.161 | 0.150 | -0.059 | -0.201 | 0.142 | -0.058 |
| 13 | 0.127 | 0.151 | 0.224 | 0.177 | 0.148 | 0.224 | 0.212 | 0.141 | 0.224 |
| 14 | -0.124 | 0.136 | 0.053 | -0.168 | 0.134 | 0.052 | -0.197 | 0.129 | 0.052 |
| 15 | 0.115 | 0.133 | -0.178 | 0.152 | 0.134 | -0.180 | 0.173 | 0.129 | -0.180 |

L refers to the longitudinal branch, and T_1 and T_2 to the transverse branches.

TABLE 10(b)

Body-centred cubic lattice, $\beta = 0$

| | $\sigma = 0.3$ | | | $\sigma = 0.4$ | | | $\sigma = 0.5$ | | |
|----|----------------|--------|--------|----------------|--------|--------|----------------|--------|--------|
| n | L | T_1 | T_2 | L | T_1 | T_2 | L | T_1 | T_2 |
| 1 | 1.065 | 1.530 | 1.630 | 1.103 | 1.629 | 1.591 | 1.131 | 1.686 | 1.531 |
| 2 | -1.145 | 0.948 | -0.415 | -1.202 | 0.712 | -0.524 | -1.242 | 0.397 | -0.589 |
| 3 | 1.133 | 0.223 | -0.228 | 1.167 | -0.175 | -0.036 | 1.176 | -0.476 | 0.129 |
| 4 | -0.934 | -0.244 | 0.329 | -0.912 | -0.426 | 0.205 | -0.864 | -0.330 | 0.025 |
| 5 | 0.688 | -0.256 | -0.023 | 0.593 | -0.133 | -0.076 | 0.489 | 0.178 | 0.034 |
| 6 | -0.398 | -0.154 | -0.088 | -0.243 | 0.120 | 0.089 | -0.109 | 0.271 | 0.088 |
| 7 | 0.159 | 0.026 | 0.110 | -0.024 | 0.224 | -0.059 | -0.144 | 0.054 | -0.166 |
| 8 | 0.031 | 0.121 | -0.080 | 0.201 | 0.083 | -0.038 | 0.271 | -0.178 | 0.132 |
| 9 | -0.135 | 0.129 | 0.064 | -0.254 | -0.067 | 0.169 | -0.261 | -0.097 | 0.012 |
| 10 | 0.180 | 0.036 | 0.052 | 0.230 | -0.110 | -0.122 | 0.189 | 0.091 | -0.054 |
| 11 | -0.161 | -0.020 | -0.107 | -0.147 | -0.005 | 0.013 | -0.090 | 0.127 | 0.056 |
| 12 | 0.117 | -0.034 | 0.048 | 0.061 | 0.061 | 0.058 | 0.017 | -0.021 | -0.056 |
| 13 | -0.056 | 0.002 | 0.002 | 0.011 | 0.053 | -0.038 | 0.031 | -0.081 | 0.088 |
| 14 | 0.012 | 0.012 | -0.096 | -0.045 | -0.007 | 0.038 | -0.052 | -0.018 | -0.053 |
| 15 | 0.014 | 0.012 | 0.029 | 0.053 | -0.020 | -0.028 | 0.070 | 0.063 | 0.000 |

L refers to the longitudinal branch, and T_1 and T_2 to the transverse branches.

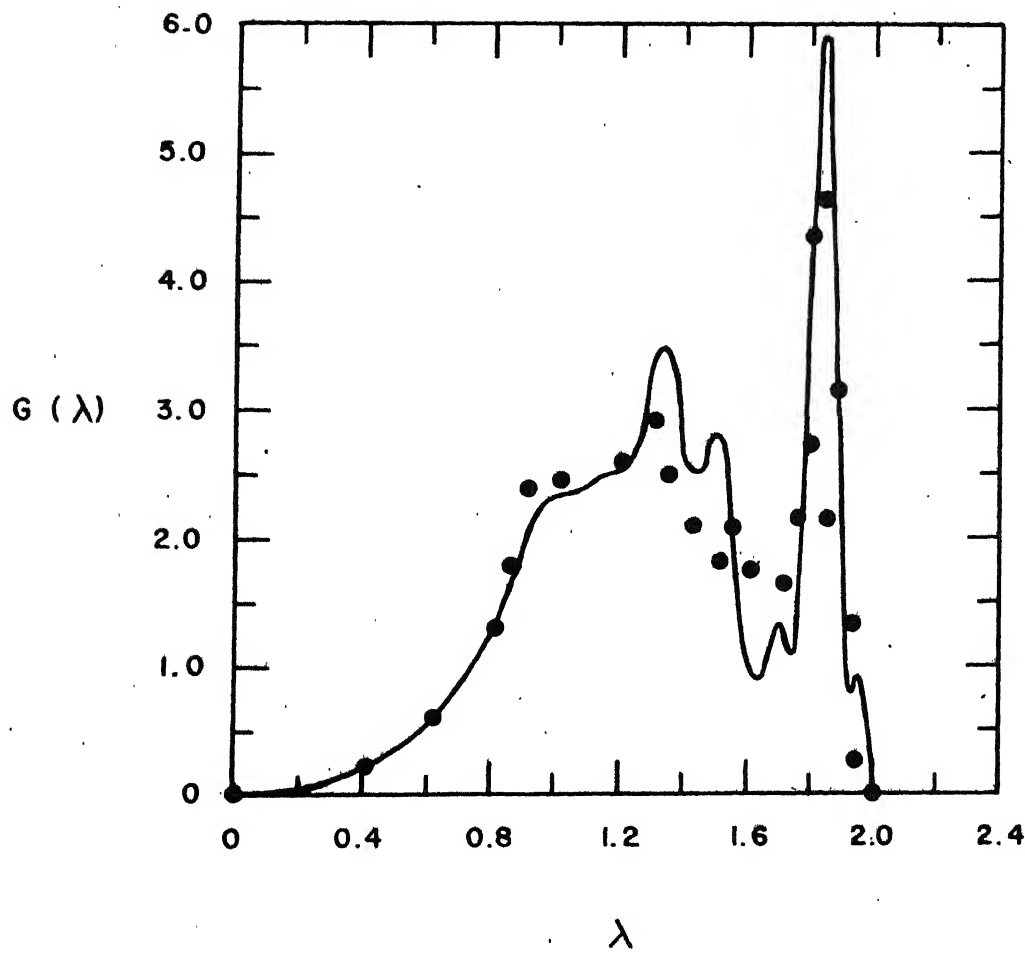


FIG. 6 FREQUENCY DISTRIBUTION FUNCTION $G(\lambda)$ OF A F. C. C. LATTICE MODEL WITH $\sigma = -0.10$. THE SOLID CURVE REPRESENTS THE PRESENT CALCULATION, AND THE CIRCLES SHOW THE RESULTS OBTAINED BY OVERTON AND DENT. HERE $\lambda^2 = M\omega^2/2\alpha$.

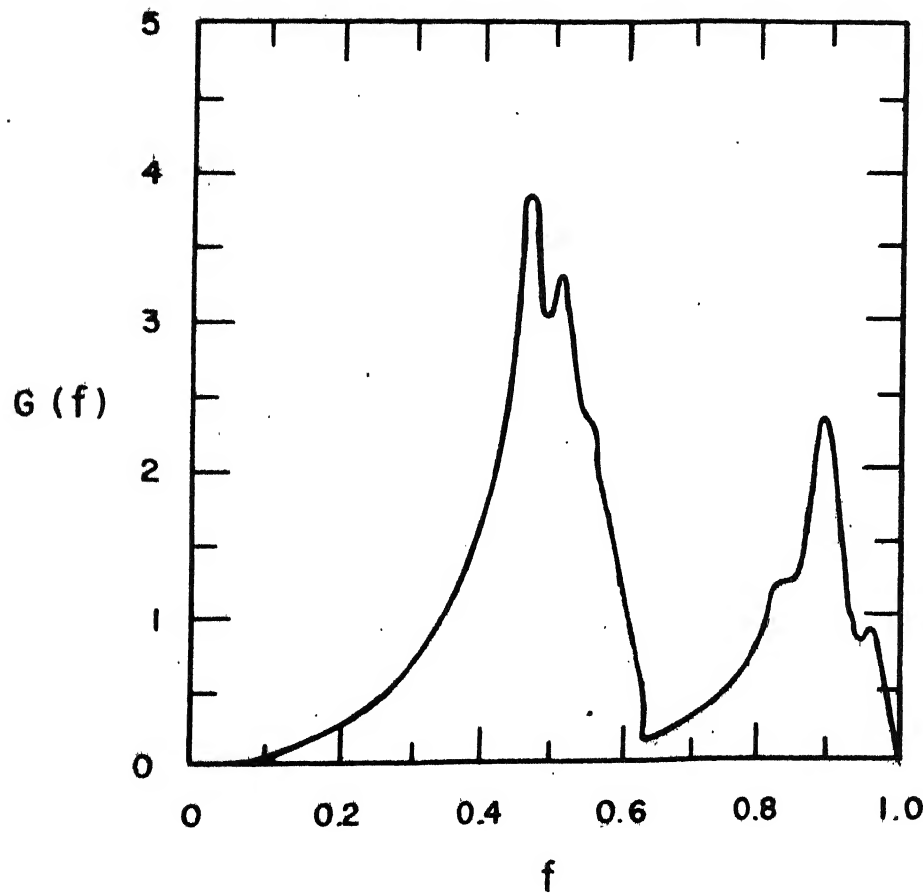


FIG. 7 FREQUENCY DISTRIBUTION FUNCTION $G(f)$ OF VANADIUM TAKING THE NONCENTRAL FORCE MODEL. f IS THE NORMALISED FREQUENCY, ω/ω_{\max} .

is expressed in a Fourier series with the number of terms in the series limited to the maximum value of n given in the tables. It may be mentioned that the machine time needed for computing the coefficients for one model was about one minute.

The frequency distribution function $G(\lambda)$ for $\sigma = - .10$ in a face-centred cubic lattice is compared with the calculations of Overton and Dent in figure 6. The agreement, in general, is quite satisfactory.

The distribution function of vanadium has also been computed by using the elastic constants given by Alers¹⁰⁷ and is plotted in figure 7. Our results are in qualitative agreement with those obtained by Hendricks et al.¹⁰⁸ using the root sampling method.

8. Remark on the Fourier Expansion Method

The method for calculating the frequency distribution function of a crystal presented above has two distinct advantages over the conventional root sampling method - a very considerable economy of time and numerical work, and yielding simple analytic expressions for the distribution function which can conveniently be used in computation of quantities that require the distribution function. The accuracy of the method can be enhanced by increasing the number of terms in the series and at the same time using a finer mesh for the integration involved in equation(69). This method does not require a close examination of the topology of the constant frequency surfaces, particularly the points of degeneracy where two or more branches cross. The methods of Gilat and Dolling and Gilat and Haubenheimer require prior knowledge of these points

of degeneracy in \mathbf{k} space.

The convergence of the Fourier series is much better than the corresponding series in Legendre polynomials. However the number of terms one must retain to get a satisfactory representation of $G(X)$ in a given case is best determined by trial. The extreme complexity of the dispersion relations makes it difficult to establish rules on this point. We have found that 15 to 20 terms give quite satisfactory results. The convergence of the Fourier series for the longitudinal branch is poorer than that for a transverse branch because of the peaking that occurs in the former in the high frequency end of the spectrum.

Since a finite Fourier series can never reproduce the critical points exactly, the question of how closely can the location of the critical points be determined by this method is of some interest. The critical points in $G(X)$ are usually such that they lead to δ -function singularities in $G''(X)$. If one first evaluates $G(X)$ with sufficient accuracy i.e. by keeping an adequate number of terms in the Fourier series such that convergence has become obvious in the form of the smallness of the last few coefficients, $G''(X)$ can then be evaluated in the form of the series,

$$G''(X) = -\pi^2 \sum_n n^2 A_n \sin(n\pi X).$$

Due to the poor convergence of the Fourier series at the critical points, as we have seen in the case of a three-dimensional simple cubic model, we shall generally get a peak of finite width instead of δ -function type singularity at such a point. Therefore,

the most one can say is that the critical point lies within the width of the prominent peak.

It remains to say something as to the law of decrease of the successive terms in the Fourier series expansion. It is evident at once that the values of the coefficients A_n must ultimately vanish indefinitely as n increases, owing to the more and more rapid fluctuation in the sign of $\sin(n\pi X)$ and the consequent more complete cancellation of the various elements in the definite integrals for the coefficients. Generally if a function $f(X)$ is continuous and its derivative has a finite number of isolated discontinuities (in a period), the convergence is ultimately as¹⁰³

$$1, \frac{1}{2^2}, \frac{1}{3^2}, \frac{1}{4^2}, \frac{1}{5^2} \dots \dots \dots$$

The distribution function for any physical three dimensional lattice is known to be continuous. A finite number of discontinuities occur only in the derivative of $G(X)$. Therefore, the convergence of the sine series expansion for $G(X)$ is the same as stated above.

Recently Mahanty¹²¹ has suggested a method to evaluate the lattice Green functions using a Fourier series expansion of their imaginary part which is related to the real part by a simple dispersion relation. The method has proved to be much faster than the direct integration of the Green function integrals and has the added advantage of yielding analytic expressions for the real and imaginary parts of the Green functions.

Having established the usefulness of the Fourier series

expansion method, we proceed to apply it to the case of diamond in the following chapter.

CHAPTER IV

APPLICATION OF THE FOURIER SERIES EXPANSION METHOD TO DIAMOND

1. Frequency Distribution Function

The elements of the dynamical matrix for a Born-von Karman model with interactions upto second neighbours were obtained in Chapter II. The values of the six force constants as obtained by different methods have been shown in Table 6. Smith⁷³ was the first to calculate the frequency distribution function of diamond (two neighbour Born-von Karman model) with the force constants which she had determined from Raman frequency and the elastic constants C_{11} and C_{12} . The frequencies of the normal modes in the (100) and (111) directions with Smith's force constants have been found to be nowhere near the experimental values from neutron scattering results⁷². Though the force constants calculated by Saint James do not yield better agreement, the distribution function has been obtained for each set of force constants calculated by him and the force constants calculated in Chapter II, in order to see the effect of variation in force constants.

The integration in equation(69) is done through the irreducible part of the first Brillouin zone which is the same as for a f.c.c. lattice and hence the same procedure of integration is adopted. The dynamical matrix now is of order 6 and has complex elements and, therefore, the diagonalisation consumes more time. It may be pointed out that one can do away the need to know the maximum frequencies in the various branches, which probably appears essential from the analysis of the Fourier series expansion method.

This is due to the fact that one can always consider the distribution function, with zero value, to exist outside the allowed band. Therefore, if ω is normalised with respect to any arbitrary frequency ω_a , taking care that ω_a is not less than the maximum frequency of the allowed band, then the Fourier expansion method will lead to a function which represents $G(X)$ inside the allowed band and has oscillations, with small amplitudes about the X-axis outside the band. $G(X)$ can be truncated at a point where these oscillations start. This fact was made use of in the case of diamond.

The initial guess for ω_{\max} is the frequency of the optical phonon at $q = 0$, which is 2.51×10^{14} rad/sec. The arbitrary frequency, therefore, is chosen to be 3×10^{14} rad/sec. to be on the safer side.

The coefficients for the first 30 terms in the Fourier series are given in Table 11, and the corresponding distribution functions are plotted in Figure 8.

The shape of the distribution curve, in each one of the four cases studied here, is very much different from the one obtained by Smith⁷³, so much so that we get four peaks in the spectrum as against only two peaks occurring in the later case. Smith had considered only central interactions with the second neighbours and calculated the spectrum by root sampling method by taking only 29 points in the irreducible part of the zone. It may not be irrelevant to mention that the spectrum for Ge and Si, which was calculated by Cole and Kineke¹¹⁰, also shows four peaks.

TABLE 11

Coefficients of the 30 terms of sine series
(force constants used are from table 6)

| n | I | II | III | IV |
|----|--------|--------|--------|--------|
| 1 | 25.168 | 26.045 | 25.101 | 24.681 |
| 2 | 5.897 | 3.724 | 7.705 | 4.771 |
| 3 | -1.912 | -3.641 | -2.601 | -2.590 |
| 4 | 5.916 | 6.097 | 4.820 | 12.006 |
| 5 | -0.035 | -1.156 | 2.463 | 3.724 |
| 6 | -1.428 | -2.756 | 0.273 | -5.808 |
| 7 | 1.142 | 1.250 | 0.210 | 3.326 |
| 8 | -0.171 | 0.100 | -1.077 | 2.536 |
| 9 | 0.491 | -0.311 | 0.892 | -5.225 |
| 10 | -2.904 | -1.397 | -1.450 | -0.904 |
| 11 | 0.950 | 2.064 | -1.907 | 3.573 |
| 12 | 5.007 | 2.928 | 3.277 | -0.256 |
| 13 | -1.845 | -3.092 | 1.228 | -2.776 |
| 14 | -2.417 | -0.248 | -1.970 | 0.048 |
| 15 | 2.264 | 2.651 | -0.222 | 1.871 |
| 16 | 0.985 | -1.305 | 0.660 | -0.093 |
| 17 | 0.426 | -0.517 | 2.130 | -0.079 |
| 18 | -0.908 | 0.186 | 0.860 | 1.055 |
| 19 | -0.997 | -0.100 | -2.161 | -0.723 |
| 20 | 1.639 | 0.823 | 0.146 | 0.478 |
| 21 | -0.939 | -0.928 | 1.137 | 2.644 |
| 22 | -0.885 | 0.626 | -0.467 | -1.117 |
| 23 | 2.052 | 1.511 | 0.239 | -2.077 |
| 24 | -0.705 | -1.759 | -0.306 | 1.760 |
| 25 | -0.751 | -0.050 | -0.367 | 0.555 |
| 26 | 1.117 | 1.298 | 0.613 | -1.315 |
| 27 | -0.048 | -0.596 | -0.542 | 0.735 |
| 28 | 0.478 | -0.039 | 0.265 | 0.114 |
| 29 | -0.266 | -0.490 | 1.209 | -1.400 |
| 30 | -0.520 | -0.085 | -0.600 | 0.449 |

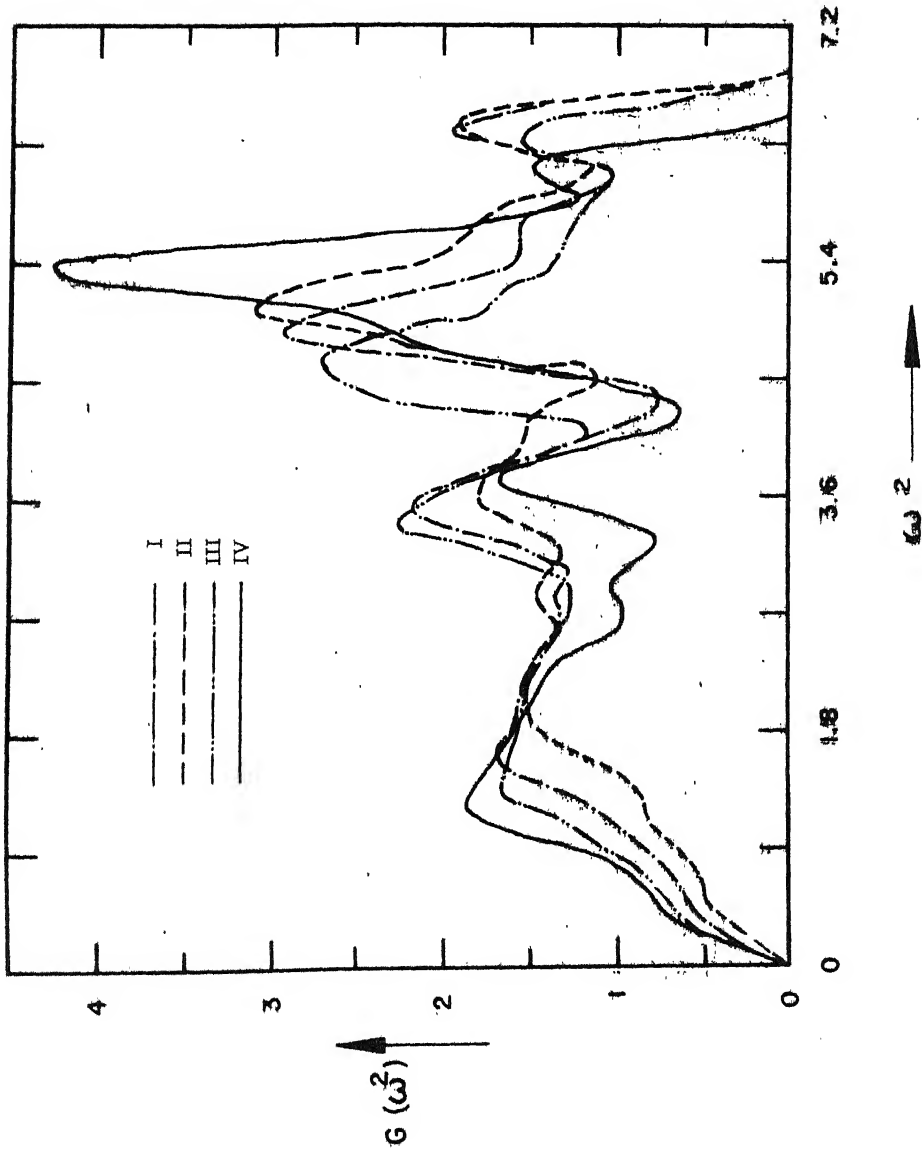


FIG. 8 $G(\omega^2)$ OF DIAMOND USING THE VARIOUS SETS OF FORCE CONSTANTS FROM TABLE 6.

One important difference among the various curves in fig.8 is the value of the maximum frequency. For curve IV it is 2.55×10^{14} rad/sec as against the value 2.60×10^{14} rad/sec for the other three curves. This is probably due to the finite value of β in the former case. It appears from Fig. 8 that the distribution curve is very sensitive to the parameter β .

2. Specific Heat

If $G(X)$ is the distribution of the squared frequencies of normal modes of a crystal, the specific heat at constant volume of 1 mole is

$$C_V = 3NK_B \int_0^{X_L} G(X) E \left(\frac{\hbar \omega}{K_B T} \right) dX , \quad (81)$$

where $X = \omega^2 / \omega_a^2$, $N =$ Avogadro's number, K_B = Boltzmann constant, \hbar = Planck's constant, T = Absolute temperature, $\omega_a = 3 \times 10^{14}$ rad/sec and $E(y)$ is given by

$$E(y) = y^2 e^y / (e^y - 1)^2 \quad . \quad (82)$$

$G(X)$ is normalised so that the integral over the entire spectrum is unity. The integral in equation(81) is solved numerically for various values of T , using all the four distribution functions. The experimental values of the specific heat of diamond have been obtained by Nernst ¹¹¹, Robertson et al. ¹¹³ and Pitzer ¹¹⁴ in the temperature range 70 - 300 K. Comparison of the theoretical and experimental values of specific heat is made in figure 9. It is evident that I and II sets of force constants do not give accurate results, whereas III and IV sets produce values of the specific heat in close agreement

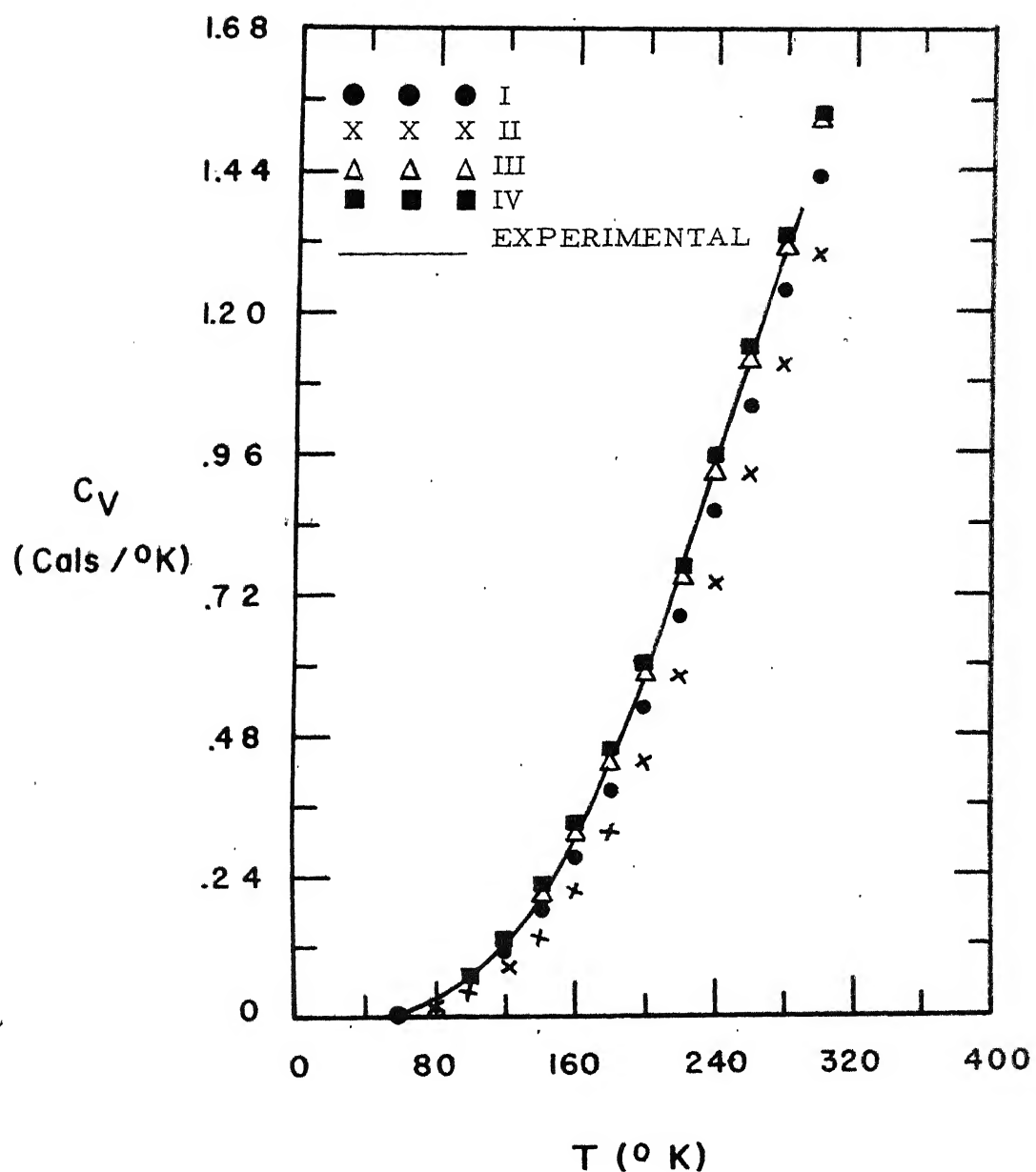


FIG. 9 SPECIFIC HEAT OF DIAMOND USING THE VARIOUS PHONON SPECTRA FROM FIG. 8.

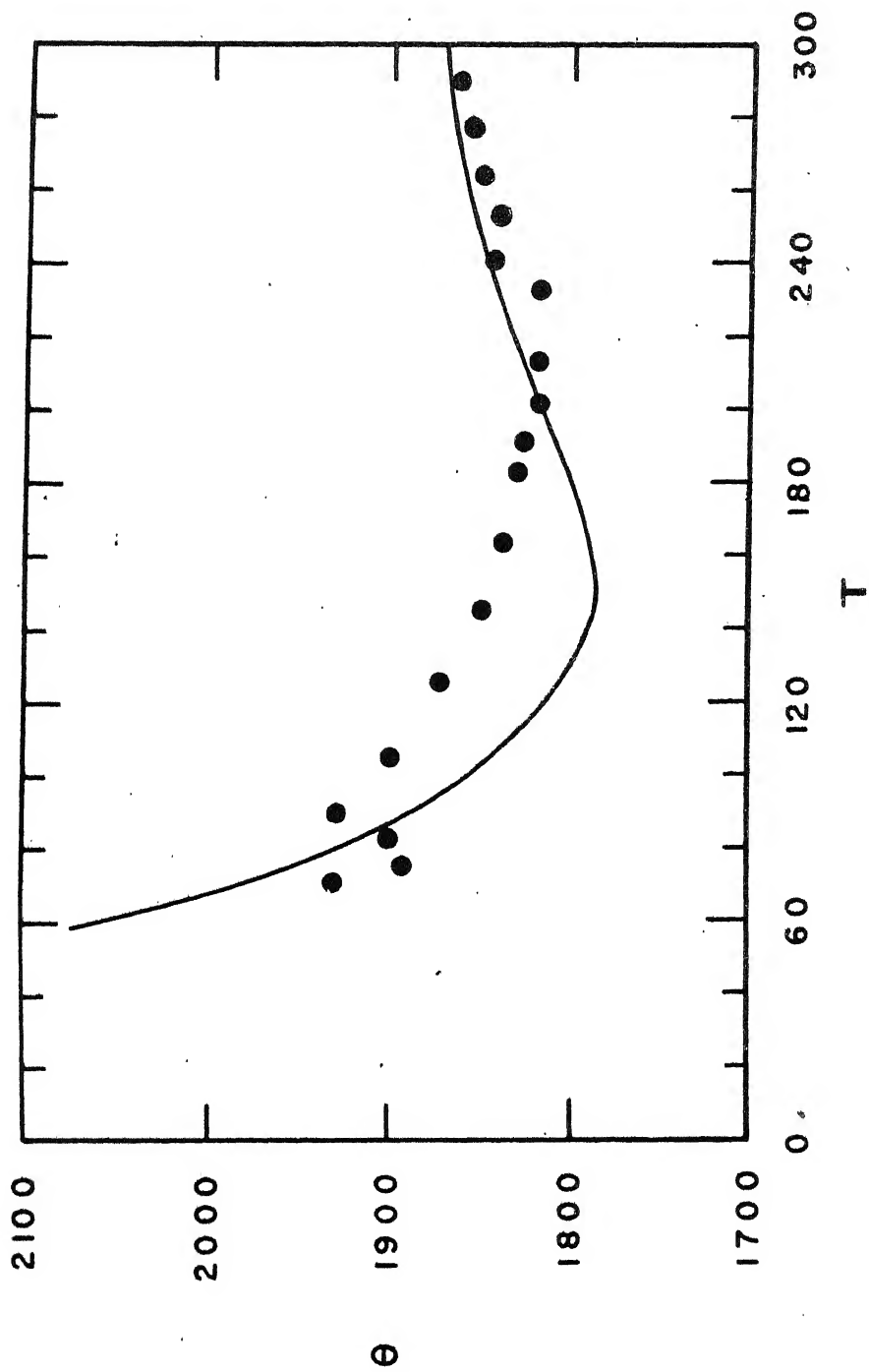


FIG. 10 TEMPERATURE DEPENDENCE OF Θ . THE CONTINUOUS CURVE IS THE RESULT OF CALCULATION USING THE PHONON SPECTRUM IV; AND THE POINTS REPRESENT THE EXPERIMENTAL DATA.

with the experimental values. Figure 10 shows the relation between the experimental and theoretical values (for model IV) of the characteristic temperature Θ .

3. Localised Modes

In pure diamond the first order dipole moment associated with any phonon is zero by symmetry. The introduction of an impurity with non-zero effective charge leads to absorption by creation of single phonons. The presence of the impurity modifies the normal modes of the perfect lattice, particularly in its vicinity. Hence the vibrational amplitude and therefore the dipole moment associated with the impurity atom are not the same as those calculated by using the unperturbed displacements. The absorption spectrum is thus characteristic of the impurity concerned. In the case of local modes, where the atomic displacements are confined to the vicinity of the impurity, this effect predominates in determining the absorption spectrum. Dawber and Elliott^{115,116} have treated the case of a substitutional charged impurity atom of mass M without any change of force constants. They show that for the case of nonatomic cubic and diamond structure materials containing a mass defect, the frequencies of the perturbed modes are given by

$$1 = \epsilon z \int_0^X \frac{G(x) dx}{z - x} , \quad (83)$$

where $z = \omega^2 / \omega_a^2$ gives the squared frequency of the perturbed modes and $x = \omega^2(k) / \omega_a^2$ gives the squared frequency of the perfect lattice modes whose normalised density of state is $G(x)$. ϵ measures

change in mass, $(M - M')/M$. The solutions of equation(83) are of two kinds according as Z lies outside or inside the region of unperturbed frequencies $\omega_j(k)$ which range from 0 to a maximum value ω_L .

For a light substitutional impurity one triply degenerate mode may lie outside the region of frequencies allowed in the perfect lattice. Such a mode is called a localised mode. We shall concern ourselves only with such modes. The value of ϵ above which a localised mode may occur, called the critical mass, depends on the shape of the distribution function used.

¹¹⁷
Angriss et al. have analysed the absorption spectrum of Si - containing boron in great detail and have found good agreement with Dawber and Elliott's theory.

We calculate here the localised mode frequencies for various values of the mass defect on the basis of the theory of Dawber and Elliott, using different frequency spectra of diamond.

If we substitute the Fourier series for $G(X)$ in equation(83), we obtain

$$\begin{aligned}
 1 &= \epsilon z \sum_n A_n \int_0^{x_L} \frac{\sin(n\pi x)}{z - x} dx \\
 &= \epsilon z \sum_n A_n \left[\cos(n\pi z) \left\{ -Si(n\pi z) + Si(n\pi(z - x_L)) \right\} \right. \\
 &\quad \left. - \sin(n\pi z) \left\{ Ci(n\pi z) + Ci(n\pi(z - x_L)) \right\} \right], \quad (84)
 \end{aligned}$$

where $Si(y)$ and $Ci(y)$ are defined as

$$Si(y) = \int_0^y \frac{\sin t}{t} dt$$

$$Ci(y) = - \int_y^\infty \frac{\cos t}{t} dt \quad (85)$$

Extensive tables for the Si and Ci functions exist (e.g. see ref.79).

The amplitude of the defect atom, $\chi(0)$, is ¹¹⁶

$$|\chi(0)|^2 = \frac{1}{M} \left[\epsilon^2 z^2 \int_0^{x_L} \frac{G(x)dx}{(z-x)^2} - \epsilon \right]^{-1} \quad (86)$$

For the Fourier series representation of $G(x)$, equation(86) reduces to

$$M |\chi(0)|^2 = \left[\epsilon^2 z^2 \sum_n A_n \left\{ \frac{\sin n\pi x_L}{z - x_L} + n\pi \sin(n\pi z) \right. \right. \\ \times \left(Si(n\pi(z - x_L)) - Si(n\pi z) \right) \\ \left. \left. + n\pi \cos(n\pi z) \left\{ Ci(n\pi(z - x_L)) - Ci(n\pi z) \right\} - \epsilon \right\} \right]^{-1} \quad (87)$$

Figure 11 shows plots of $\left(\frac{\omega^2}{\omega_L^2} - 1 \right)$ and $M |\chi(0)|^2$ against ϵ .

It is at once clear that the curves(a) for the localised mode frequencies are quite insensitive to the finer details of the frequency spectrum. On the other hand the critical values of the mass defect parameter, ϵ_C , are very much different for the different distribution curves. Though this statement is generally true, two different

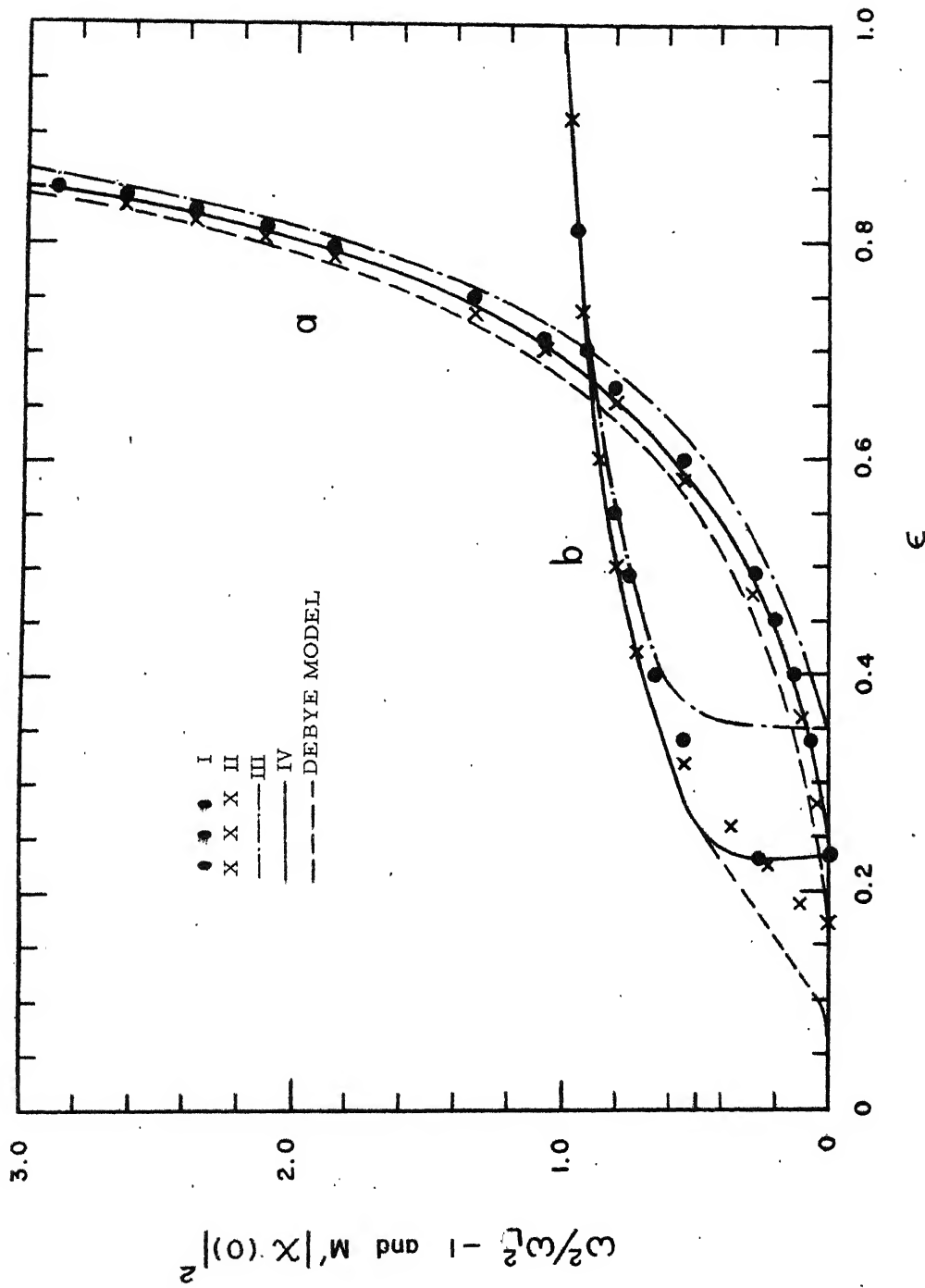


FIG. 11 (a) RELATIVE SQUARED FREQUENCY OF THE LOCAL MODE DUE TO A LIGHT MASS $0 < \epsilon < 1$ USING THE DIFFERENT PHONON SPECTRA. HERE, $\omega_0 = 3 \times 10^{14}$ rad/sec.
 (b) RELATIVE AMPLITUDE OF VIBRATION OF THE DEFECT FOR THE CORRESPONDING PHONON SPECTRUM.

distribution curves may lead to the same value of ϵ_c , which in fact is the case for curves I and IV. The values of ϵ_c for the distribution curves obtained by using I, II, III and IV sets of force constants are approximately .23, .14, .35 and .23 respectively. It may be mentioned that Angress et al.¹¹⁷ found the value of ϵ_c as $\sim .25$ for silicon, using a particular form of phonon spectrum.

The other set of curves, b, in figure 11 represents the relative amplitude of the defect atom. These curves are comparatively more sensitive to the form of the phonon spectrum for small ϵ . The properties of the local mode become increasingly less sensitive to the phonon spectrum employed as ϵ increases (which means as the impurity mass decreases). This is quite expected because the local mode frequency increases rapidly as ϵ increases towards unity and the vibrations become more concentrated round the defect, and consequently the impurity atom vibrates in virtually static surroundings.

The absorption spectrum in diamond has been observed by Robertson et al.¹¹², Sutherland et al.¹¹⁹ and Smith and Taylor¹²⁰, and the different spectra are compared by Elliott¹¹⁸ who has shown that only type I diamonds give a local mode peak at about .17 eV ($\omega \approx 2.6 \times 10^{14}$ rad/sec) just above the maximum frequency of the allowed band. This corresponds to a mass defect just above the critical mass defect parameter which is .23 for the phonon spectra I and IV in figure 9. This reflects the presence of Be⁹ isotope. The conclusion must be taken as very tentative as it is based on Dawber and Elliotts' formula(83) which is valid only for an isolated charged mass defect without any change in spring constants.

CHAPTER V

CONCLUSION

In the thesis presented above, firstly a new method based on a Fourier series expansion has been used for the evaluation of the frequency distribution function. It has been applied to a two neighbour Born-von Karman model for face-centred (with central force interactions only) and body-centred (with non-central force interactions with the first neighbours and central force interactions with the second neighbours) cubic lattices. It is found that 15 terms in the Fourier series are sufficient to obtain a reasonable representation of the frequency distribution function. The first fifteen coefficients have been evaluated for these lattices with various force constant ratios.

Secondly the lattice dynamics of diamond has been studied in detail. The simplified two neighbour Born-von Karman model (with the second neighbour interaction being limited to only central forces) that was previously studied by Smith⁷³ is found to be in disagreement with the neutron scattering data obtained recently by Warren et al.⁷² For this reason the angular and torsional forces have also been included in the interactions with the second neighbours. Such a model contains only five parameters. The three elastic constants and the Raman frequency were put as constraints for the evaluation of the force constants. Only one parameter β was allowed to vary to get the best fit with the measured frequencies at the zone boundaries in the (100) and (111) directions. When the elastic data of Bhagavantam and Bhimasenachar⁷⁶ is used, the value $\beta = .044$ is found to give a reasonably good fit with the measured dispersion curves. The deviation is generally within the experimental